Chapter 4

Analysis of Bernoulli Lines

Motivation: The problem of performance analysis of production systems consists of investigating their performance measures, e.g., production rate (PR), work-in-process (WIP_i), blockages (BL_i) and starvations (ST_i), as functions of machine and buffer parameters. In principle, this investigation can be carried out using computer simulations. However, the simulation approach has two drawbacks. First, it is not conducive to analysis of fundamental properties of production systems, e.g., relationships between system parameters and performance measures. Second, simulations require a relatively lengthy and costly process of developing a computer model and its multiple runs for statistical evaluation of the performance measures. In some cases, especially when numerous "what if" scenarios must be analyzed, this approach may become prohibitively expensive and slow. This problem is exacerbated by the exponential explosion of the dimensionality of the system as a function of buffer capacity. Indeed, even in the Bernoulli reliability case (i.e., when the machines are memoryless), a serial line with, say, 11 machines and buffers of capacity 9, has 10^{10} states, which is overwhelming for simulations. Therefore, a quick, easy and revealing method for production systems analysis, based on formulas, rather than on simulations, is of importance. The purpose of this chapter is to present such a method for serial production lines with Bernoulli machines along with describing system-theoretic properties of these systems.

Overview: The analytical approach to calculating PR, WIP_i, BL_i and ST_i is based on the mathematical models of production systems discussed in Chapter 3. Due to the complex nature of interactions among the machines, closed-form expressions for their performance measures are all but impossible to derive, except for the case of systems with two machines. Therefore, the approach, developed here, is based on a two-stage procedure: First, analytical formulas for performance analysis of two-machine lines are derived and, second, an aggregation procedure is developed, which reduces longer systems to a set of coupled two-machine lines and recursively evaluates their performance characteristics. This approach, illustrated in Figure 4.1, leads to sufficiently accurate estimates of performance measures PR, WIP_i, BL_i and ST_i.

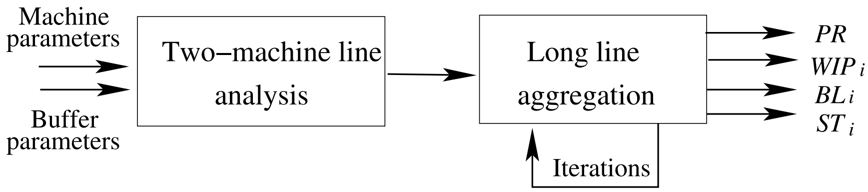

Figure 4.1: Block diagram of the analysis procedure

In addition, based on the analysis of the aggregation equations, this chapter investigates several system-theoretic properties, which provide qualitative insights into the behavior of serial lines.

4.1 Two-machine Lines

4.1.1 Mathematical description

System: The production system considered here is shown in Figure 4.2. The time is slotted with slot duration equal to the cycle time of the machines, and machines m_1 and m_2 are up during each time slot with probability p_1 and p_2, respectively. The buffer is of capacity $N < \infty$.

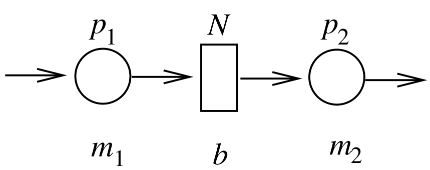

Figure 4.2: Two-machine Bernoulli production line

States of the system: Since the Bernoulli machines are memoryless, the states of the system coincide with the states of the buffer, i.e., the state space consists of $N + 1$ points: $0, 1, \ldots, N$.

Conventions: The following conventions are used to define the system at hand:

(a) Blocked before service.
(b) The first machine is never starved; the last machine is never blocked.
(c) The status of the machines is determined at the beginning and the state of the buffer at the end of each time slot.
(d) Each machine status is determined independently from the other.

(e) Time-dependent failures.

State transition diagram: Since the buffer occupancy can change in each time slot at most by one part, the state transition diagram is "linear," as shown in Figure 4.3.

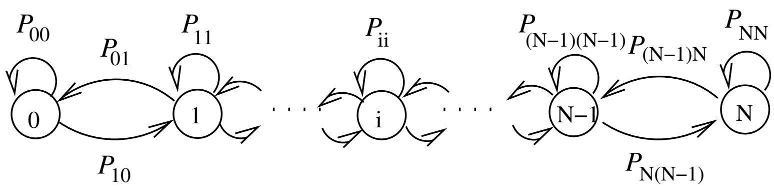

Figure 4.3: Transition diagram of two-machine Bernoulli production line

Transition probabilities: In the expressions that follow, the events $\{m_i$ is up during the time slot $n+1\}$ and $\{m_i$ is down during the time slot $n+1\}$ are denoted for the sake of brevity as $\{m_i \text{ up}\}$ and $\{m_i \text{ down}\}$. The buffer occupancy at slot n is denoted as $h(n)$. In these notations, the transition probabilities are:

$$
\begin{aligned}
P_{00} &= P[h(n+1)=0|h(n)=0] = P[\{m_1 \text{ down}\}], \\
P_{01} &= P[h(n+1)=0|h(n)=1] = P[\{m_1 \text{ down}\} \cap \{m_2 \text{ up}\}], \\
P_{10} &= P[h(n+1)=1|h(n)=0] = P[\{m_1 \text{ up}\}], \\
\cdots & \quad \cdots \quad \cdots \quad \cdots \quad \cdots \\
P_{ii} &= P[h(n+1)=i|h(n)=i] = P[(\{m_1 \text{ up}\} \cap \{m_2 \text{ up}\}) \\
&\quad \cup(\{m_1 \text{ down}\} \cap \{m_2 \text{ down}\})], \quad i=1,\ldots,N-1, \\
P_{i(i+1)} &= P[h(n+1)=i|h(n)=i+1] = P[\{m_1 \text{ down}\} \cap \{m_2 \text{ up}\}], \\
&\qquad i=1,\ldots,N-1, \\
P_{(i+1)i} &= P[h(n+1)=i+1|h(n)=i] = P[\{m_1 \text{ up}\} \cap \{m_2 \text{ down}\}], \\
&\qquad i=1,\ldots,N-1, \\
\cdots & \quad \cdots \quad \cdots \quad \cdots \quad \cdots \\
P_{NN} &= P[h(n+1)=N|h(n)=N] = P[(\{m_1 \text{ up}\} \cap \{m_2 \text{ up}\}) \\
&\quad \cup\{m_2 \text{ down}\}].
\end{aligned}
$$

Using the formulas for the probability of the union of mutually exclusive events (2.1) and for the probability of the intersection of independent events (2.3), these transition probabilities can be calculated as follows:

$$\begin{aligned}
P_{00} &= P[\{m_1 \text{ down}\}] = 1 - p_1, \\
P_{01} &= P[\{m_1 \text{ down}\} \cap \{m_2 \text{ up}\}] = (1-p_1)p_2, \\
P_{10} &= P[\{m_1 \text{ up}\}] = p_1, \\
\cdots & \quad \cdots \quad \cdots \quad \cdots \quad \cdots \\
P_{ii} &= P[\{m_1 \text{ up}\}]P[\{m_2 \text{ up}\}] + P[\{m_1 \text{ down}\}]P[\{m_2 \text{ down}\}] \\
&= p_1p_2 + (1-p_1)(1-p_2), \qquad i = 1, \ldots, N-1, \\
P_{i(i+1)} &= P[(\{m_1 \text{ down}\}]P[\{m_2 \text{ up}\})] \\
&= (1-p_1)p_2, \qquad i = 1, \ldots, N-1, \\
P_{(i+1)i} &= P[(\{m_1 \text{ up}\}]P[\{m_2 \text{ down}\})] \\
&= p_1(1-p_2), \qquad i = 1, \ldots, N-1, \\
\cdots & \quad \cdots \quad \cdots \quad \cdots \quad \cdots \\
P_{NN} &= P[\{m_1 \text{ up}\}]P[\{m_2 \text{ up}\}] + P[\{m_2 \text{ down}\}] \\
&= p_1p_2 + 1 - p_2.
\end{aligned} \tag{4.1}$$

Dynamics of the system: Since the transition probabilities (4.1) are constant, the system under consideration is a Markov chain. Let $P_i(n)$ be the probability of state i, $i = 0, 1, \ldots, N$, at time n. Then, as it is shown in Subsection 2.3.3, the evolution of $P_i(n)$ can be described by the following constrained linear dynamical system:

$$P_i(n+1) = \sum_{j=0}^{N} P_{ij}P_j(n), \qquad i = 0, 1, \ldots, N, \tag{4.2}$$

$$\sum_{i=0}^{N} P_i(n) = 1. \tag{4.3}$$

Statics of the system: The steady state of the system at hand is described by the balance equations

$$P_i = \sum_{j=0}^{N} P_{ij}P_j, \qquad i = 0, 1, \ldots, N, \tag{4.4}$$

$$\sum_{i=0}^{N} P_i = 1. \tag{4.5}$$

Their solution provides a complete characterization of the system behavior. This is accomplished next.

4.1.2 Steady state probabilities

Since the states are communicating and there are "self-loops" (see Figure 4.3), the Markov chain (4.1) is ergodic. Therefore, there exists a unique stationary probability mass function. Taking into account (4.1), the balance equations can be re-written as

$$\begin{array}{rcl}
P_0 & = & (1-p_1)P_0 + (1-p_1)p_2P_1, \\
P_1 & = & p_1P_0 + [p_1p_2 + (1-p_1)(1-p_2)]P_1 + (1-p_1)p_2P_2, \\
\cdots & & \cdots \quad \cdots \quad \cdots \quad \cdots \\
P_i & = & p_1(1-p_2)P_{i-1} + [p_1p_2 + (1-p_1)(1-p_2)]P_i \\
 & & +(1-p_1)p_2P_{i+1}, \qquad\qquad i = 2,\ldots,N-1, \\
\cdots & & \cdots \quad \cdots \quad \cdots \quad \cdots \\
P_N & = & p_1(1-p_2)P_{N-1} + (p_1p_2 + 1 - p_2)P_N.
\end{array} \tag{4.6}$$

These equations can be solved consecutively in terms of P_0. Indeed, from the first equation in (4.6) we have

$$P_1 = \frac{p_1}{(1-p_1)p_2}P_0.$$

It is convenient to re-write this expression as

$$P_1 = \Big(\frac{1}{1-p_2}\Big)\Big(\frac{p_1(1-p_2)}{p_2(1-p_1)}\Big)P_0$$

and denote the second factor in the right hand side as

$$\alpha(p_1,p_2) := \frac{p_1(1-p_2)}{p_2(1-p_1)}. \tag{4.7}$$

Then, from the second equation of (4.6),

$$P_2 = \Big(\frac{1}{1-p_2}\Big)\Big(\frac{p_1(1-p_2)}{p_2(1-p_1)}\Big)^2 P_0 = \frac{\alpha^2(p_1,p_2)}{1-p_2}P_0$$

and so on, leading to

$$P_N = \frac{\alpha^N}{1-p_2}P_0,$$

where, for the sake of brevity, $\alpha(p_1,p_2)$ is denoted as α. Thus,

$$P_i = \frac{\alpha^i}{1-p_2}P_0, \qquad i = 1,\ldots,N. \tag{4.8}$$

To complete the calculation, the expression for P_0 must be derived. Using (4.5) and (4.8), we obtain

$$P_0\Big[1 + \frac{\alpha}{1-p_2} + \frac{\alpha^2}{1-p_2} + \ldots + \frac{\alpha^N}{1-p_2}\Big] = 1.$$

Thus,

$$P_0 = \frac{1-p_2}{1-p_2+\alpha+\alpha^2+\ldots+\alpha^N}. \tag{4.9}$$

In the special case of identical machines, i.e., when $p_1 = p_2 =: p$,

$$\alpha(p_1, p_2) = 1,$$

and, therefore,

$$P_0 = \frac{1-p}{N+1-p}, \tag{4.10}$$

implying that

$$P_i = \frac{1}{N+1-p}, \qquad i = 1, \dots, N. \tag{4.11}$$

An illustration of the pmf (4.10), (4.11) is given in Figure 4.4 for $p = 0.95$ and $p = 0.55$ with $N = 5$. Clearly, when p is close to 1 (which is the practical case),

$$\begin{aligned} P_i &\approxeq \frac{1}{N}, \qquad i = 1, \dots, N, \\ P_0 &\approxeq 0. \end{aligned}$$

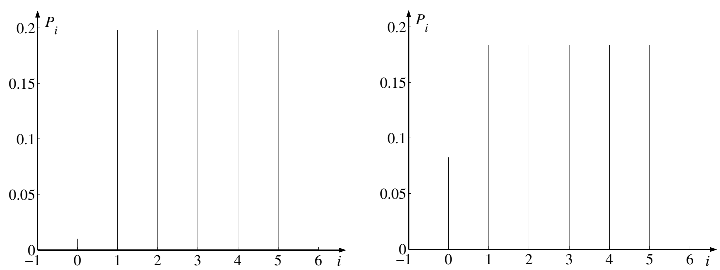

(a) $p_1 = p_2 = 0.95, N = 5$ (b) $p_1 = p_2 = 0.55, N = 5$

Figure 4.4: Stationary pmf of buffer occupancy in two-machine lines with identical Bernoulli machines

Intuitively, one would expect that the pmf of the buffer occupancy in the case $p_1 = p_2$ would be symmetric in the sense that $P_0 = P_N$. The fact that it is not is due to the blocked before service assumption, i.e., m_1 is not blocked even if $h = N$ but m_2 is up. If this assumption is changed to "m_1 is blocked if $h = N$" (i.e., irrespective of the status of m_2), it is possible to show that the buffer occupancy is indeed symmetric, i.e., $P_0 = P_N$ (see Problem 4.5). We follow, however, the original assumption since it is closer to reality on the factory floor. (Note that in the case of continuous time systems, discussed in Part III, both assumptions lead to the same conclusion – the pdf of buffer occupancy for the case of identical machines is symmetric.)

When $p_1 \neq p_2$, substituting (4.7) into (4.9) we obtain:

$$P_0 = \frac{1-p_2}{1-p_2 + \frac{p_1(1-p_2)}{p_2(1-p_1)}\left(1+\alpha+\alpha^2+\ldots+\alpha^{N-1}\right)}.$$

Summing up the geometric series in the denominator, this can be re-written as

$$P_0 = \frac{1-p_2}{1-p_2+\frac{p_1(1-p_2)}{p_2(1-p_1)}\cdot\frac{1-\alpha^N}{1-\alpha}} = \frac{1}{1+\frac{p_1}{(1-p_1)p_2}\cdot\frac{1-\alpha^N}{1-\alpha}},$$

i.e.,

$$P_0 = \frac{(1-p_1)(1-\alpha)}{(1-p_1)(1-\alpha)+\frac{p_1}{p_2}(1-\alpha^N)}.$$

Substituting (4.7) into the first term in the denominator of the above expression, after simplification we finally obtain:

$$P_0 = \frac{(1-p_1)(1-\alpha)}{1-\frac{p_1}{p_2}\alpha^N}. \tag{4.12}$$

Thus, equations (4.8), (4.12) describe the steady state pmf of buffer occupancy in two-machine lines with non-identical Bernoulli machines. This pmf is illustrated in Figure 4.5 for the following serial lines:

$$\begin{aligned} L_1: &\quad p_1 = 0.8, p_2 = 0.82, N = 5,\\ L_2: &\quad p_1 = 0.82, p_2 = 0.8, N = 5,\\ L_3: &\quad p_1 = 0.6, p_2 = 0.9, N = 5,\\ L_4: &\quad p_1 = 0.9, p_2 = 0.6, N = 5. \end{aligned} \tag{4.13}$$

Clearly, L_1 and L_2 are a reverse of each other, in the sense that the first (respectively, second) machine of L_1 is the second (respectively, first) machine of L_2, while the buffer remains the same. Similarly, L_3 and L_4 are also reverse of each other. The pmf's of Figure 4.5 clearly show that the buffer tends to be empty (respectively, full) if $p_1 - p_2 < 0$ (respectively, $p_1 - p_2 > 0$), and this phenomenon becomes more pronounced when $|p_1 - p_2|$ is large.

The functions in the right hand side of (4.10) and (4.12) play an important role in the subsequent analyses. Similar functions appear in all other cases of serial lines (e.g., when the machines are exponential). Therefore, we introduce a special notation:

$$Q(p_1,p_2,N) := P_0 = \begin{cases} \frac{(1-p_1)(1-\alpha(p_1,p_2))}{1-\frac{p_1}{p_2}\alpha^N(p_1,p_2)}, & \text{if } p_1 \neq p_2,\\ \\ \frac{1-p}{N+1-p}, & \text{if } p_1 = p_2 = p. \end{cases} \tag{4.14}$$

The properties of this function are as follows:

Lemma 4.1 *Function* $Q(x,y,N)$*, where* $0 < x < 1$*,* $0 < y < 1$*, and* $N \in \{1,2,\ldots\}$*, takes values on* $(0,1)$ *and is*

- *strictly decreasing in* x*,*
- *strictly increasing in* y*,*
- *strictly decreasing in* N*.*

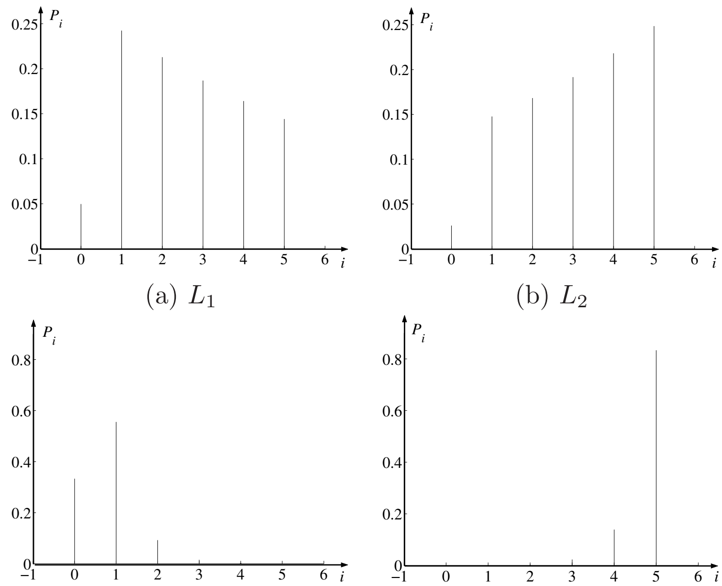

(a) L_1 (b) L_2

(c) L_3 (d) L_4

Figure 4.5: Stationary pmf of buffer occupancy in two-machine lines with non-identical Bernoulli machines

Proof: See Section 20.1.

The properties of Q, as indicated in Section 4.2, ensure the convergence of the aggregation procedure that is used for analysis of serial lines with more than two machines.

To conclude this subsection, we re-write the expression for the probability of the buffer being full (i.e., P_N) in a form, which is more convenient for the performance measure formulas described in Subsection 4.1.3.

From (4.8) and (4.12) we obtain

$$P_N = \frac{(1-p_1)(1-\alpha(p_1,p_2))\alpha^N(p_1,p_2)}{(1-p_2)(1-\frac{p_1}{p_2}\alpha^N(p_1,p_2))}.$$

Dividing both numerator and denominator by α^N and replacing $\frac{p_2(1-p_1)}{p_1(1-p_2)}$ with $\frac{1}{\alpha}$, after simplification, we obtain

$$P_N = \frac{1-\frac{1}{\alpha(p_1,p_2)}}{1-\frac{p_2}{p_1}(\frac{1}{\alpha(p_1,p_2)})^N}. \tag{4.15}$$

Taking into account that, as it follows from (4.7),

$$\frac{1}{\alpha(p_1,p_2)} = \alpha(p_2,p_1),$$

this, finally, can be re-written as

$$P_N = \frac{1-\alpha(p_2,p_1)}{1-\frac{p_2}{p_1}\alpha^N(p_2,p_1)}. \tag{4.16}$$

4.1.3 Formulas for the performance measures

Using the steady state probabilities derived above and function Q defined by (4.14), the performance measures PR, WIP, BL_1, and ST_2 can be expressed as shown below.

Production rate: Keeping in mind conventions (a)-(e) listed at the beginning of this section and formula (2.3) for the probability of the intersection of independent events, PR can be represented as

$$\begin{aligned} PR &= P[\{m_2 \text{ is up at the beginning of a time slot}\} \cap \{\text{buffer is not empty} \\ &\qquad \text{at the end of the previous time slot}\}] \\ &= P[\{m_2 \text{ up}\}]P[\{\text{buffer not empty}\}] \\ &= p_2(1-P_0) \\ &= p_2[1-Q(p_1,p_2,N)]. \end{aligned} \tag{4.17}$$

Alternatively, PR can be expressed as

$$\begin{aligned} PR &= P[\{m_1 \text{ is up at the beginning of a time slot}\} \cap \{\text{buffer is not full at} \\ &\qquad \text{the beginning of this time slot}\}]. \end{aligned} \tag{4.18}$$

While the probability of the first event in the right hand side of (4.18) is p_1, the probability of the second event is

$$\begin{aligned} &P[\{\text{buffer is not full at the beginning of a time slot}] \\ &\quad = 1 - P[\{\text{buffer is full at the end of the previous slot}\} \\ &\qquad \cap\{m_2 \text{ is down at the beginning of this time slot}\}] \\ &\quad = 1 - P_N(1-p_2). \end{aligned}$$

Therefore,

$$PR = p_1[1-(1-p_2)P_N],$$

where, as it follows from (4.11) and (4.16),

$$P_N = \begin{cases} \frac{1-\alpha(p_2,p_1)}{1-\frac{p_2}{p_1}\alpha^N(p_2,p_1)}, & \text{if } p_1 \neq p_2, \\ \\ \frac{1}{N+1-p}, & \text{if } p_1 = p_2 = p. \end{cases}$$

This implies that

$$(1-p_2)P_N = Q(p_2,p_1,N),$$

and, therefore,

$$PR = p_1[1 - Q(p_2, p_1, N)].$$

Thus, PR can be expressed in two equivalent ways:

$$\begin{aligned} PR &= p_1[1 - Q(p_2, p_1, N)] \\ &= p_2[1 - Q(p_1, p_2, N)]. \end{aligned} \tag{4.19}$$

These are important expressions: along with their direct value as PR of two-machine lines, they are the basis of the aggregation procedure for the analysis of $M > 2$-machine lines (see Section 4.2).

Work-in-process: The average value of pmf's (4.10), (4.11) and (4.8), (4.12), i.e., WIP, is given by

$$WIP = \sum_{i=1}^{N} iP_i = \sum_{i=1}^{N} \frac{i\alpha^i}{1 - p_2} Q(p_1, p_2, N). \tag{4.20}$$

For $p_1 = p_2 = p$, this leads to

$$WIP = \frac{1}{N + 1 - p} \sum_{i=1}^{N} i = \frac{N(N + 1)}{2(N + 1 - p)}. \tag{4.21}$$

For $p_1 \neq p_2$, after some algebraic manipulations, this can be reduced to

$$WIP = \frac{p_1}{p_2 - p_1\alpha^N(p_1, p_2)} \Big[\frac{1 - \alpha^N(p_1, p_2)}{1 - \alpha(p_1, p_2)} - N\alpha^N(p_1, p_2)\Big]. \tag{4.22}$$

Therefore,

$$WIP = \begin{cases} \frac{p_1}{p_2 - p_1\alpha^N(p_1,p_2)} \Big[\frac{1-\alpha^N(p_1,p_2)}{1-\alpha(p_1,p_2)} - N\alpha^N(p_1, p_2)\Big], & \text{if } p_1 \neq p_2, \\ \frac{N(N+1)}{2(N+1-p)}, & \text{if } p_1 = p_2 = p. \end{cases} \tag{4.23}$$

Blockages and starvations: As it follows from the definitions of Subsection 3.6.3,

$$\begin{aligned} BL_1 &= P[\{m_1 \text{ up}\} \cap \{\text{buffer full}\} \cap \{m_2 \text{ down}\}], \\ ST_2 &= P[\{m_2 \text{ up}\} \cap \{\text{buffer empty}\}]. \end{aligned}$$

Taking into account that the probabilities of the buffer being full, P_N, and being empty, P_0, are given by (4.16) and (4.14), respectively, these relationships can be expressed as

$$\begin{aligned} BL_1 &= p_1P_N(1 - p_2) = p_1Q(p_2, p_1, N), \\ ST_2 &= p_2P_0 = p_2Q(p_1, p_2, N). \end{aligned} \tag{4.24}$$

Clearly, these expressions are in agreement with formulas (4.19) for PR, which now can be understood as

$$\begin{aligned} PR &= p_1 - BL_1 \\ &= p_2 - ST_2. \end{aligned}$$

4.1.4 Asymptotic properties

Expressions (4.19), (4.23) and (4.24) reveal the following properties of the performance measures as $N \to \infty$:

Theorem 4.1 *In a two-machine line with Bernoulli machines defined by conventions (a)-(e),*

$$\lim_{N\to\infty} PR = \min(p_1, p_2), \tag{4.25}$$

$$\lim_{N\to\infty} WIP = \begin{cases} \infty, & \text{if } p_1 > p_2, \\ \frac{p_1(1-p_1)}{p_2-p_1}, & \text{if } p_1 < p_2, \\ \lim_{N\to\infty} \frac{N}{2} = \infty, & \text{if } p_1 = p_2, \end{cases} \tag{4.26}$$

$$\lim_{N\to\infty} BL_1 = 0, \tag{4.27}$$

$$\lim_{N\to\infty} ST_2 = \begin{cases} 0, & \text{if } p_1 \geq p_2, \\ p_2 - p_1, & \text{if } p_1 < p_2. \end{cases} \tag{4.28}$$

Proof: See Section 20.1.

The last expression in (4.26) implies that for N sufficiently large and $p_1 = p_2$, the buffer is, on the average, half full.

Theorem 4.1 is illustrated in Figure 4.6 for three serial lines defined by

$$\begin{aligned} L_1 :&\quad p_1 = p_2 = 0.9, \\ L_2 :&\quad p_1 = 0.9, p_2 = 0.7, \\ L_3 :&\quad p_1 = 0.7, p_2 = 0.9. \end{aligned} \tag{4.29}$$

As one can see, PR is monotonically increasing but with a decreasing rate, while WIP increases linearly (if $p_1 \geq p_2$). This implies that there is nothing to be gained from having a buffer of capacity larger than 5. The issue of buffer capacity selection is explored in details in Chapter 6.

4.2 $M > 2$-machine Lines

4.2.1 Mathematical description and approach

System: The production system considered here is shown in Figure 4.7. The time is slotted, and each machine m_i, $i = 1, \dots, M$, is up during a time slot with

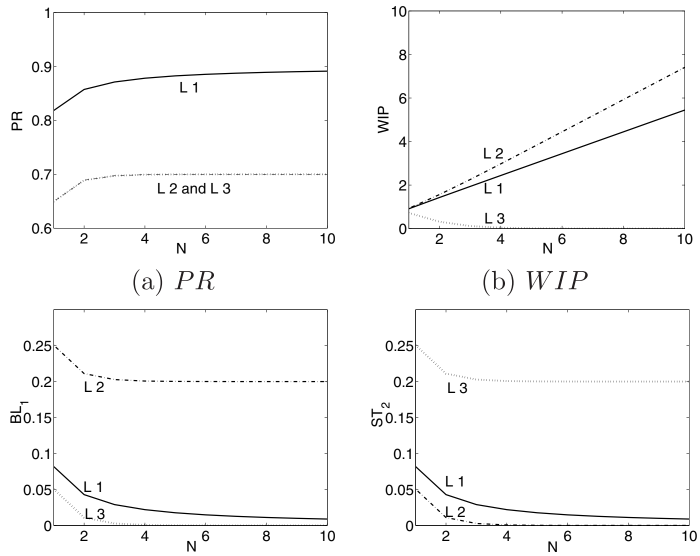

(a) PR (b) WIP

(c) BL_1 (d) ST_2

Figure 4.6: Performance measures of two-machine Bernoulli lines as functions of buffer capacity

probability p_i and down with probability $1 - p_i$, $i = 1, \dots, M$. The capacity of buffer i is $N_i < \infty$, $i = 1, \dots, M - 1$.

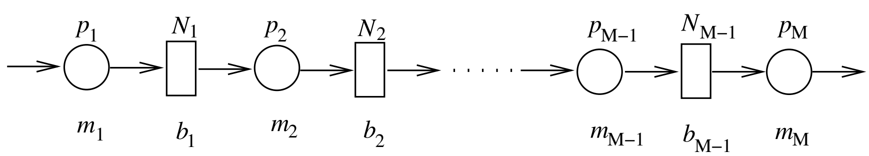

Figure 4.7: M-machine Bernoulli production line

Conventions: Similar to two-machine lines, the following conventions are used:

(a) Blocked before service.

(b) Machine m_1 is never starved for parts; machine m_M is never blocked by subsequent operations.

(c) The status of the machines is determined at the beginning, and the state of the buffers at the end of each time slot.

(d) Each machine's status is determined independently from the others.

(e) Time-dependent failures.

Throughout this book, we refer to (a)-(e) intermittently as either conventions or assumptions.

States of the system: The Bernoulli machines are memoryless, and, therefore, the states of the system coincide with the states of the buffers. Since the i-th buffer has $N_i + 1$ states, the system has $(N_1 + 1)(N_2 + 1) \cdots (N_{M-1} + 1)$ states. For example, if $N_i = 9$ for all i and $M = 23$, the number of states is 10^{22}, which equals the number of molecules in a cubic centimeter of gas under normal pressure and temperature! Clearly, a direct analysis of such a large system is impossible (and, perhaps, unnecessary as well). Therefore, a simplification is in order. We use for this purpose an aggregation approach.

Idea of the aggregation: Consider the M-machine line and aggregate the last two machines, m_{M-1}, and m_M, into a single Bernoulli machine denoted as m^b_{M-1}, where b stands for *backward* aggregation (see Figure 4.8(a)). The Bernoulli parameter, p^b_{M-1}, of this machine is assigned as the production rate of the aggregated two-machine line, calculated using the first expression of (4.19). Next, aggregate this machine, i.e., m^b_{M-1}, with m_{M-2} and obtain another aggregated machine, m^b_{M-2}. Continue this process until all the machines are aggregated into m^b_1, which completes the *backward* phase of the aggregation procedure.

It turns out that the Bernoulli parameter of m^b_1 might be quite different from the production rate of the M-machine line under consideration. To remedy this problem, we introduce the *forward* phase of the aggregation procedure defined as follows: Aggregate the first machine, m_1, with the aggregated version of the rest of the line, i.e., with m^b_2. This results in the aggregated machine, denoted as m^f_2, where f stands for *forward* aggregation (see Figure 4.8(b)). The Bernoulli parameter, p^f_2, is assigned as the production rate of the aggregated two-machine line, calculated using the second expression of (4.19) with p_2 in function Q substituted by p^b_2. Next, aggregate m^f_2 with m^b_3, resulting in m^f_3 and so on until all the machines are aggregated into m^f_M, which completes the forward phase of the procedure. Again, the Bernoulli parameter of m^f_M may be quite different from the actual production rate of the M-machine system.

To alleviate this discrepancy, we iterate between the backward and forward aggregations. In other words, view the above backward and forward aggregations as the first iteration of the aggregation, i.e., as $s = 1$. At the second iteration, $s = 2$, m^f_{M-1} is aggregated with m_M to result in m^b_{M-1} for the second iteration, which is then aggregated with m^f_{M-2} and so on until the second iteration of the backward aggregation is complete. Next, the second iteration of the forward aggregation is carried out, followed by the third iteration of the backward aggregation and so on, i.e., $s = 3, 4, \ldots$.

We show below that the steady states of this recursive procedure lead to relatively accurate estimates of the performance measures for the M-machine line. We also indicate that the convergence to these steady states is quite rapid,

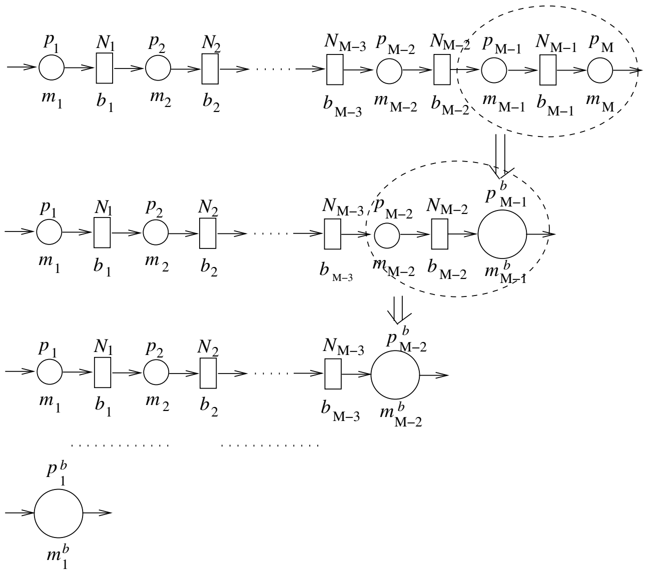

(a). Backward aggregation

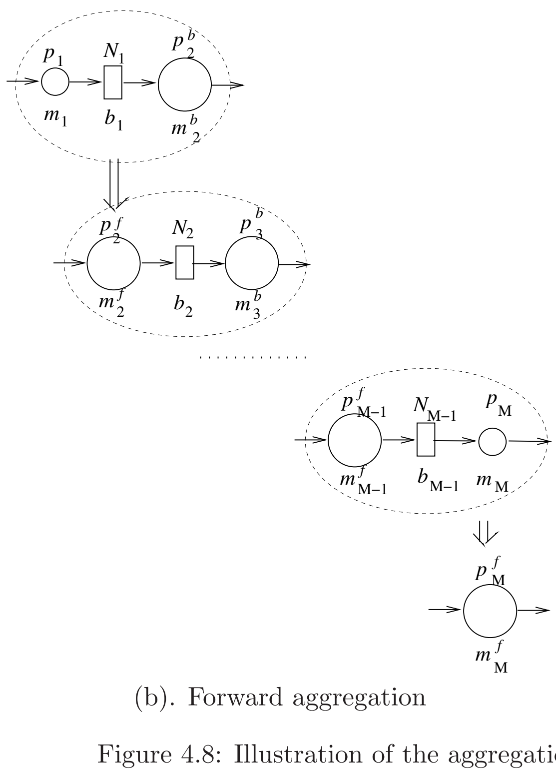

(b). Forward aggregation

Figure 4.8: Illustration of the aggregation procedure

typically requiring less than 10 iterations, which implies that the performance measures are evaluated within a fraction of a second.

4.2.2 Aggregation procedure and its properties

The mathematical representation of the recursive aggregation procedure described above and its properties are given below.

Recursive Aggregation Procedure 4.1:

$$\begin{aligned} p_i^b(s+1) &= p_i[1 - Q(p_{i+1}^b(s+1), p_i^f(s), N_i)], \\ &\qquad\qquad\qquad\qquad i = 1, \ldots, M-1, \\ p_i^f(s+1) &= p_i[1 - Q(p_{i-1}^f(s+1), p_i^b(s+1), N_{i-1})], \\ &\qquad\qquad\qquad\qquad i = 2, \ldots, M, \\ &\qquad s = 0, 1, 2, \ldots, \end{aligned} \tag{4.30}$$

with initial conditions

$$p_i^f(0) = p_i, \qquad i = 1, \ldots, M \tag{4.31}$$

and boundary conditions

$$\begin{aligned} p_1^f(s) &= p_1, \qquad s = 0, 1, 2, \ldots, \\ p_M^b(s) &= p_M, \qquad s = 0, 1, 2, \ldots. \end{aligned} \tag{4.32}$$

As before,

$$Q(x, y, N) = \begin{cases} \frac{(1-x)(1-\alpha)}{1 - \frac{x}{y}\alpha^N}, & \text{if } x \neq y, \\ \\ \frac{1-x}{N+1-x}, & \text{if } x = y, \end{cases} \tag{4.33}$$

where

$$\alpha = \frac{x(1-y)}{y(1-x)}. \tag{4.34}$$

These equations are solved as follows: With $i = M-1$, using the initial condition $p_{M-1}^f(0) = p_{M-1}$ and the boundary condition $p_M^b(s) = p_M$, solve the first equation of (4.30) to obtain $p_{M-1}^b(1)$; then solve it with $i = M-2$ to obtain $p_{M-2}^b(1)$, and so on, until $p_1^b(1)$ is obtained. Next, solve the second equation of (4.30) with $i = 2$ to obtain $p_2^f(1)$; then solve it with $i = 3$ to obtain $p_3^f(1)$ and so on, until $p_M^f(1)$ is obtained. This completes the first iteration of the aggregation procedure. For the second, third, ..., iterations, this process is repeated anew using $p_{M-1}^f(1)$, $p_{M-1}^f(2)$, ..., respectively, in the first equation of (4.30).

Example 4.1 Consider a three-machine serial line with $p = [0.9, 0.9, 0.9]$ and $N = [2, 2]$. Then,

$$
\begin{aligned}
s = 1 :& \\
p_2^b(1) &= p_2[1 - Q(p_3, p_2, N_2)] = 0.9[1 - Q(0.9, 0.9, 2)] = 0.8571, \\
p_1^b(1) &= p_1[1 - Q(p_2^b(1), p_1, N_1)] = 0.9[1 - Q(0.8571, 0.9, 2)] = 0.8257, \\
p_2^f(1) &= p_2[1 - Q(p_1, p_2^b(1), N_1)] = 0.9[1 - Q(0.9, 0.8571, 2)] = 0.8670, \\
p_3^f(1) &= p_3[1 - Q(p_2^f(1), p_3, N_2)] = 0.9[1 - Q(0.8670, 0.9, 2)] = 0.8333, \\
s = 2 :& \\
p_2^b(2) &= p_2[1 - Q(p_3, p_2^f(1), N_2)] = 0.9[1 - Q(0.9, 0.8670, 2)] = 0.8650, \\
p_1^b(2) &= p_1[1 - Q(p_2^b(2), p_1, N_1)] = 0.9[1 - Q(0.8650, 0.9, 2)] = 0.8318, \\
p_2^f(2) &= p_2[1 - Q(p_1, p_2^b(2), N_1)] = 0.9[1 - Q(0.9, 0.8650, 2)] = 0.8654, \\
p_3^f(2) &= p_3[1 - Q(p_2^f(2), p_3, N_2)] = 0.9[1 - Q(0.8654, 0.9, 2)] = 0.8321, \\
s = 3 :& \\
p_2^b(3) &= p_2[1 - Q(p_3, p_2^f(2), N_2)] = 0.9[1 - Q(0.9, 0.8654, 2)] = 0.8653, \\
p_1^b(3) &= p_1[1 - Q(p_2^b(3), p_1, N_1)] = 0.9[1 - Q(0.8653, 0.9, 2)] = 0.8320, \\
p_2^f(3) &= p_2[1 - Q(p_1, p_2^b(3), N_1)] = 0.9[1 - Q(0.9, 0.8653, 2)] = 0.8653, \\
p_3^f(3) &= p_3[1 - Q(p_2^f(3), p_3, N_2)] = 0.9[1 - Q(0.8653, 0.9, 2)] = 0.8320, \\
s = 4 :& \\
p_2^b(4) &= p_3[1 - Q(p_3, p_2^f(3), N_2)] = 0.9[1 - Q(0.9, 0.8653, 2)] = 0.8653, \\
p_1^b(4) &= p_2[1 - Q(p_2^b(4), p_1, N_1)] = 0.9[1 - Q(0.8653, 0.9, 2)] = 0.8320, \\
p_2^f(4) &= p_2[1 - Q(p_1, p_2^b(4), N_1)] = 0.9[1 - Q(0.9, 0.8653, 2)] = 0.8653, \\
p_3^f(4) &= p_3[1 - Q(p_2^f(4), p_3, N_2)] = 0.9[1 - Q(0.8653, 0.9, 2)] = 0.8320, \\
s = 5 :& \\
p_2^b(5) &= p_3[1 - Q(p_3, p_2^f(4), N_2)] = 0.9[1 - Q(0.9, 0.8653, 2)] = 0.8653, \\
p_1^b(5) &= p_2[1 - Q(p_2^b(5), p_1, N_1)] = 0.9[1 - Q(0.8653, 0.9, 2)] = 0.8320, \\
p_2^f(5) &= p_2[1 - Q(p_1, p_2^b(5), N_1)] = 0.9[1 - Q(0.9, 0.8653, 2)] = 0.8653, \\
p_3^f(5) &= p_3[1 - Q(p_2^f(5), p_3, N_2)] = 0.9[1 - Q(0.8653, 0.9, 2)] = 0.8320, \\
& \quad \ldots .
\end{aligned}
$$

All subsequent iterations are carried out similarly.

Convergence: Clearly, (4.30) is an $(M-1)$-dimensional dynamical system, which iterates p_i's and N_i's and results in two sequences of numbers

$$
\begin{aligned}
&p_1^b(s), \ldots, p_{M-1}^b(s), \\
&p_2^f(s), \ldots, p_M^f(s), \\
&\qquad s = 1, 2, \ldots
\end{aligned}
$$

defined on the interval $(0,1)$. The properties of these sequences and their physical meaning are described below.

Based on (4.30) and Lemma 4.1, the following can be proved:

Theorem 4.2 *Aggregation procedure (4.30)-(4.33) has the following properties:*

(i) The sequences, $p_2^f(s), \ldots, p_M^f(s)$ *and* $p_1^b(s), \ldots, p_{M-1}^b(s)$, $s = 1, 2, \ldots$, *are convergent, i.e., the following limits exist:*

$$\begin{aligned} p_i^b &:= \lim_{s\to\infty} p_i^b(s), \\ p_i^f &:= \lim_{s\to\infty} p_i^f(s). \end{aligned} \tag{4.35}$$

(ii) These limits are unique solutions of the steady state equations corresponding to (4.30), i.e., of

$$\begin{aligned} p_i^f &= p_i[1 - Q(p_{i-1}^f, p_i^b, N_{i-1})], \qquad 2 \le i \le M, \\ p_i^b &= p_i[1 - Q(p_{i+1}^b, p_i^f, N_i)], \qquad 1 \le i \le M-1, \\ & p_1^f = p_1, \qquad p_M^b = p_M. \end{aligned}$$

(iii) In addition, these limits satisfy the relationships:

$$\begin{aligned} p_M^f &= p_1^b \\ &= p_{i+1}^b[1 - Q(p_i^f, p_{i+1}^b, N_i)] \\ &= p_i^f[1 - Q(p_{i+1}^b, p_i^f, N_i)], \qquad i = 1, \ldots, M-1. \end{aligned}$$

Proof: See Section 20.1.

Figure 4.9 illustrates the behavior of $p_i^f(s)$ and $p_i^b(s)$, $s = 0, 1, 2, \ldots$, for the following lines:

$$\begin{aligned} L_1: &\qquad p_i = 0.9, i = 1, \ldots, 5; N_i = 3, i = 1, \ldots, 4, \\ L_2: &\qquad p = [0.7, 0.75, 0.8, 0.85, 0.9], N_i = 3, i = 1, \ldots, 4, \\ L_3: &\qquad p = [0.7, 0.85, 0.9, 0.85, 0.7], N_i = 3, i = 1, \ldots, 4, \\ L_4: &\qquad p = [0.9, 0.85, 0.7, 0.85, 0.9], N_i = 3, i = 1, \ldots, 4. \end{aligned}$$

Obviously, L_1 represents lines with identical machines, while L_2, L_3, and L_4 illustrate lines where p_i's are allocated according to an increasing, inverted bowl, and bowl patterns, respectively. As one can see, p_i^f and p_i^b indeed exhibit the properties established in Theorem 4.2. In addition, Figure 4.9 shows that convergence to the limits is quite fast: 2 - 4 iterations of the aggregation procedure for the uniform, ramp, and bowl allocations and about 15 iterations for the inverted bowl.

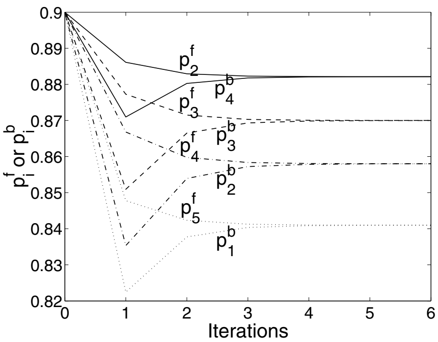

(a) L_1

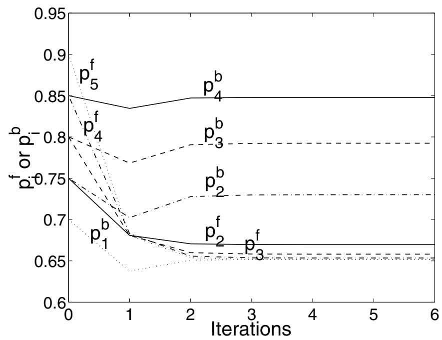

(b) L_2

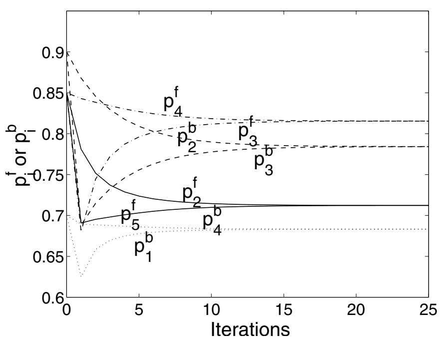

(a) L_3

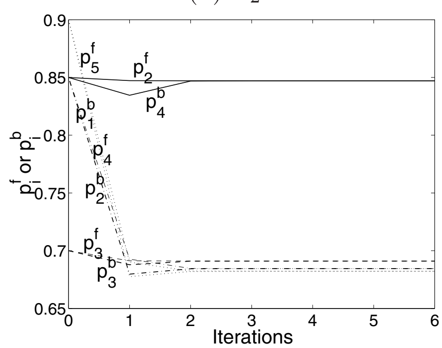

(b) L_4

Figure 4.9: Illustration of the dynamics of $p_i^f(s)$ and $p_i^b(s)$

Interpretation: As it follows from statement (iii) of Theorem 4.2, p_i^f and p_i^b can be given the following interpretation: From the point of view of each buffer b_i, $i = 1, \ldots, M-1$, the upstream of the line is represented by the "virtual" Bernoulli machine m_i^f defined by the parameter p_i^f. Similarly, the downstream is represented by the "virtual" machine m_{i+1}^b defined by p_{i+1}^b. In addition, the whole line can be represented by m_1^b or m_M^f. Thus, the M-machine line can be represented as shown in Figure 4.10. Clearly, all the performance measures of the two-machine lines included in this figure can be calculated using the formulas of Subsection 4.1.3.

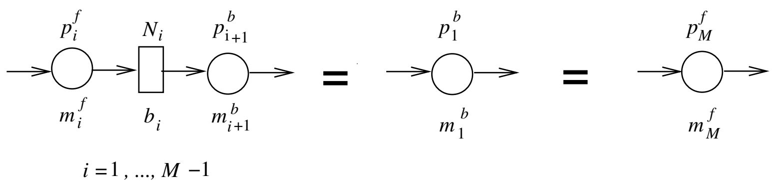

Figure 4.10: Equivalent representations of Bernoulli $M > 2$-machine line through the aggregated machines.

4.2.3 Formulas for the performance measures

Using the equivalent representations of Figure 4.10 and the limits (4.35), estimates of the performance measures of the $M > 2$-machine line are introduced below.

Production rate: Based on Figure 4.10 and Theorem 4.2, the estimate, $\widehat{PR}$, of the production rate is defined as

$$\begin{aligned} \widehat{PR} &= p_1^b = p_M^f \\ &= p_{i+1}^b[1 - Q(p_i^f, p_{i+1}^b, N_i)] \\ &= p_i^f[1 - Q(p_{i+1}^b, p_i^f, N_i)], \\ & \quad i = 1, \ldots, M-1. \end{aligned} \tag{4.36}$$

Work-in-process: Using the two-machine representation of the $M > 2$-machine line (Figure 4.10) and expression (4.23), the estimate, $\widehat{WIP}_i$, of the steady state occupancy of buffer i is defined as

$$\widehat{WIP}_i = \begin{cases} \frac{p_i^f}{p_{i+1}^b - p_i^f \alpha^{N_i}(p_i^f, p_{i+1}^b)} \Big[\frac{1-\alpha^{N_i}(p_i^f, p_{i+1}^b)}{1-\alpha(p_i^f, p_{i+1}^b)} - N_i \alpha^{N_i}(p_i^f, p_{i+1}^b) \Big], & \text{if } p_i^f \neq p_{i+1}^b, \\ \frac{N_i(N_i+1)}{2(N_i+1-p_i^f)}, & \text{if } p_i^f = p_{i+1}^b. \end{cases} \tag{4.37}$$
$$i = 1, \ldots, M-1.$$

Obviously, the estimate of the total WIP is

$$\widehat{WIP} = \sum_{i=1}^{M-1} \widehat{WIP}_i. \tag{4.38}$$

Blockages and starvations: Since these probabilities must evaluate blockages and starvations of the real, rather then aggregated, machines, taking into account expressions (4.24), the estimates of these performance measures, $\widehat{BL}_i$ and $\widehat{ST}_i$, are introduced as follows:

$$\begin{aligned} \widehat{BL}_i &= p_i Q(p^b_{i+1}, p^f_i, N_i), \qquad i = 1, \dots, M-1, &(4.39)\\ \widehat{ST}_i &= p_i Q(p^f_{i-1}, p^b_i, N_{i-1}), \qquad i = 2, \dots, M. &(4.40) \end{aligned}$$

These expressions confirm the interpretation of p^f_i and p^b_i described in the aggregation procedure. Indeed, using the steady states of the aggregation procedure (4.30) and expressions (4.39), (4.40), we obtain

$$\begin{aligned} p^b_i &= p_i[1 - Q(p^b_{i+1}, p^f_i, N_i)] \\ &= p_i - \widehat{BL}_i, &(4.41)\\ p^f_i &= p_i[1 - Q(p^f_{i-1}, p^b_i, N_{i-1})] \\ &= p_i - \widehat{ST}_i. &(4.42) \end{aligned}$$

Residence time: Given $\widehat{PR}$ and $\widehat{WIP}$, an estimate of RT can be calculated as follows:

$$\widehat{RT} = \frac{\widehat{WIP}}{\widehat{PR}}[\text{cycle time}].$$

PSE Toolbox: The recursive procedure (4.30) and performance measure estimates (4.36)-(4.40) are implemented in the **Performance Analysis** function of the toolbox. For a description and illustration of this tool, see Subsection 19.3.1.

4.2.4 Asymptotic properties of $M > 2$-machine lines

Formulas (4.36)-(4.40) can be used to investigate asymptotic properties of Bernoulli lines as $N \to \infty$. This is carried out using the following eight serial lines:

$$\begin{aligned}
L_1: &\quad p_i = 0.9, i = 1, \dots, 5, N_i = N, i = 1, \dots, 4,\\
L_2: &\quad p = [0.9, 0.85, 0.8, 0.75, 0.7], N_i = N, i = 1, \dots, 4,\\
L_3: &\quad p = [0.7, 0.75, 0.8, 0.85, 0.9], N_i = N, i = 1, \dots, 4,\\
L_4: &\quad p = [0.9, 0.85, 0.7, 0.85, 0.9], N_i = N, i = 1, \dots, 4,\\
L_5: &\quad p = [0.7, 0.85, 0.9, 0.85, 0.7], N_i = N, i = 1, \dots, 4,\\
L_6: &\quad p = [0.7, 0.9, 0.7, 0.9, 0.7], N_i = N, i = 1, \dots, 4,\\
L_7: &\quad p = [0.9, 0.7, 0.9, 0.7, 0.9], N_i = N, i = 1, \dots, 4,\\
L_8: &\quad p = [0.75, 0.75, 0.95, 0.75, 0.75], N_i = N, i = 1, \dots, 4.
\end{aligned} \tag{4.43}$$

The reasons for selecting these particular lines are as follows: Line 1 illustrates the behavior of systems with identical machines. Lines 2 and 3 represent systems with increasing and decreasing machine efficiency, respectively; clearly, L_3 is the reverse of L_2. Lines 4 and 5 illustrate systems with machine efficiency allocated according to a bowl and an inverted bowl patterns, respectively. Lines 6 and 7 exemplify systems with "oscillating" machine efficiency allocation. Finally, Line 8 is selected to illustrate the case of a good machine surrounded by low efficiency ones.

Figures 4.11 - 4.18 show the performance measures of these lines as a function of N. Based on this information, the following can be concluded: As $N \to \infty$,

- $\widehat{PR} \to \min p_i$, $i = 1, \dots, 5$.
- $\widehat{WIP}_i$, $i = 1, \dots, 4$, are increasing almost linearly in N, with $\widehat{WIP}_i \cong \kappa_i N$, $\kappa_4 < \dots < \kappa_1 < 1$, when p_i's form a decreasing sequence.
- $\widehat{WIP}_i$, $i = 1, \dots, 4$, are also increasing almost linearly but with smaller coefficients κ_i, so that $\widehat{WIP}_i \cong \kappa_i N$, $\kappa_4 < \dots < \kappa_1 < 1$, when p_i's are identical.
- $\widehat{WIP}_i$, $i = 1, \dots, 4$, converges to a finite limit with $\widehat{WIP}_i > \widehat{WIP}_{i-1}$, $i = 2, 3, 4$, when p_i's form an increasing sequence.

In addition, Figures 4.11 - 4.18 indicate that since $\widehat{PR}$ as a function of N exhibits saturation, while $\sum_i WIP_i$ tends to infinity (except for the case of increasing machine efficiency), there is no reason for having large N, typically, above 8 - 10. A detailed discussion on selecting N is included in Chapter 6.

4.2.5 Accuracy of the estimates

Clearly, formulas (4.36)-(4.40) are just estimates of the true values of the performance measures. Therefore, an analysis of their accuracy is of importance. In this subsection, such an analysis is carried out using both analytical and numerical tools.

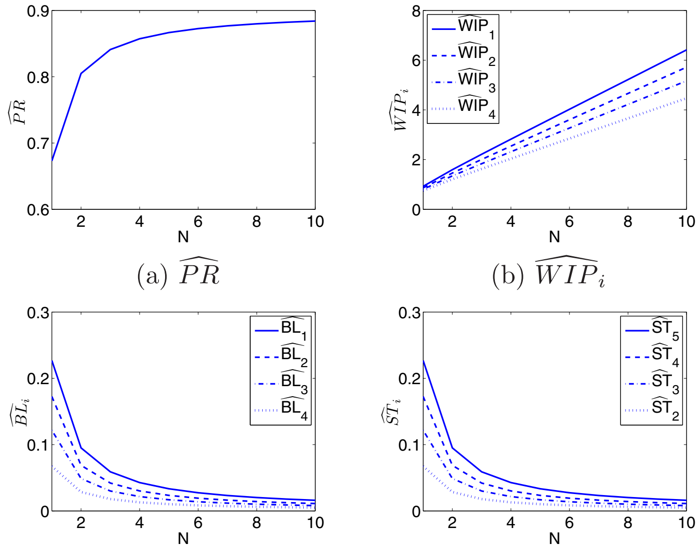

(a) $\widehat{PR}$ (b) $\widehat{WIP}_i$

(c) $\widehat{BL}_i$ (d) $\widehat{ST}_i$

Figure 4.11: Performance of Line L_1 (identical machines)

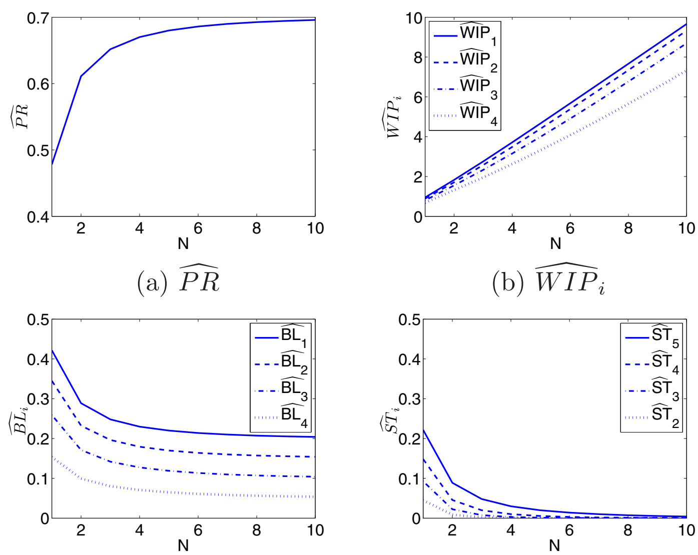

(a) $\widehat{PR}$ (b) $\widehat{WIP}_i$

(c) $\widehat{BL}_i$ (d) $\widehat{ST}_i$

Figure 4.12: Performance of Line L_2 (decreasing machine efficiency)

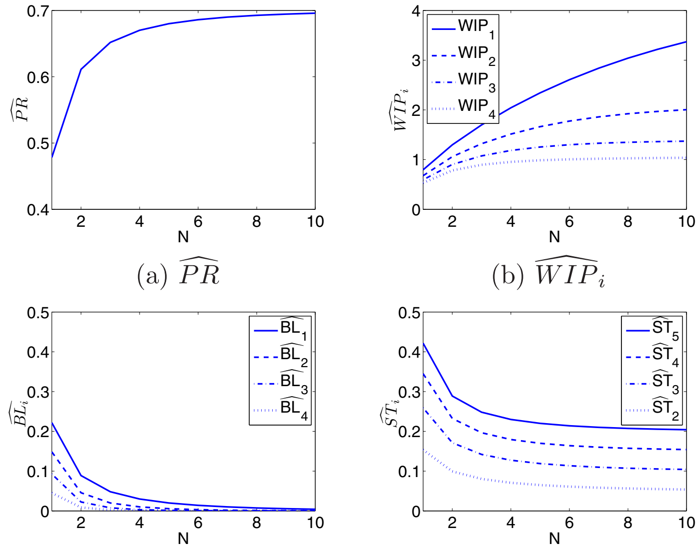

(a) $\widehat{PR}$ (b) $\widehat{WIP}_i$

(c) $\widehat{BL}_i$ (d) $\widehat{ST}_i$

Figure 4.13: Performance of Line L_3 (increasing machine efficiency)

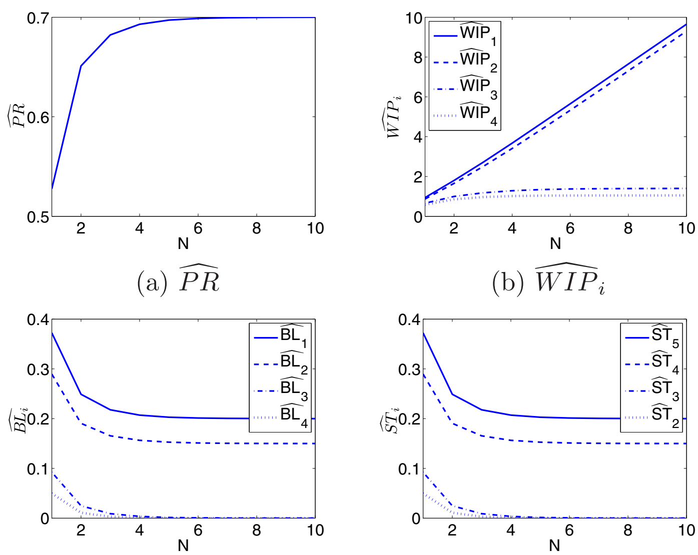

(a) $\widehat{PR}$ (b) $\widehat{WIP}_i$

(c) $\widehat{BL}_i$ (d) $\widehat{ST}_i$

Figure 4.14: Performance of Line L_4 (bowl machine efficiency allocation)

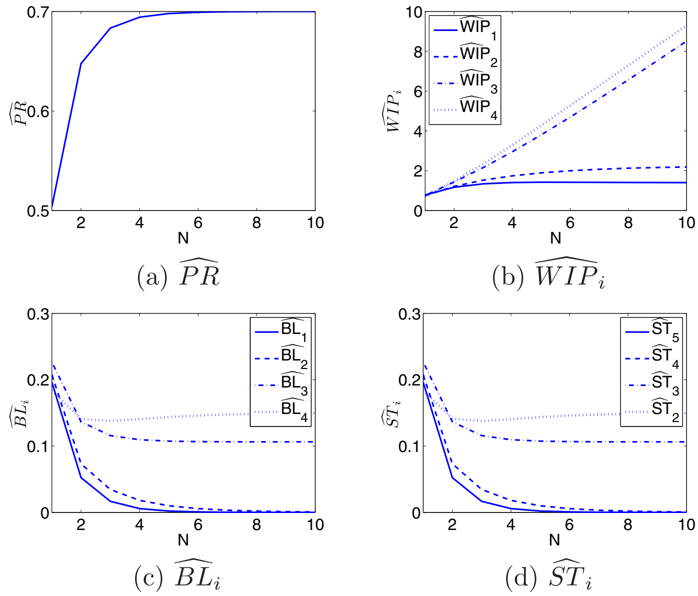

(a) $\widehat{PR}$ (b) $\widehat{WIP}_i$

(c) $\widehat{BL}_i$ (d) $\widehat{ST}_i$

Figure 4.15: Performance of Line L_5 (inverted bowl machine efficiency allocation)

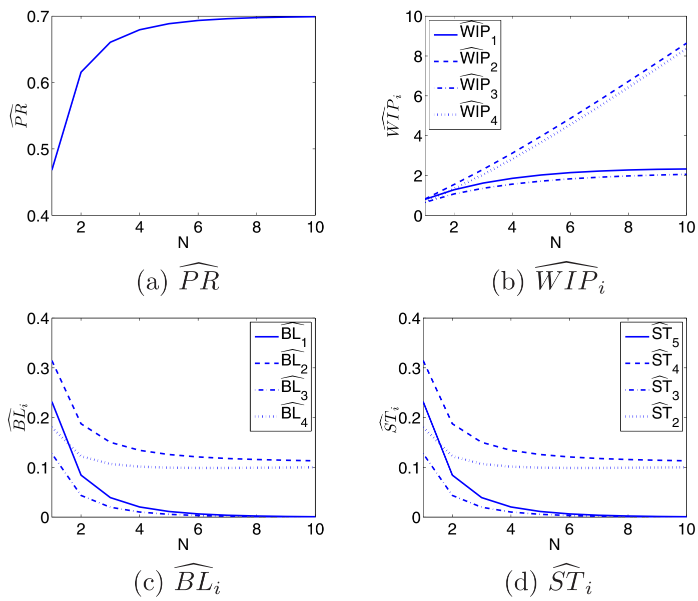

(a) $\widehat{PR}$ (b) $\widehat{WIP}_i$

(c) $\widehat{BL}_i$ (d) $\widehat{ST}_i$

Figure 4.16: Performance of Line L_6 (“oscillating” machine efficiency allocation)

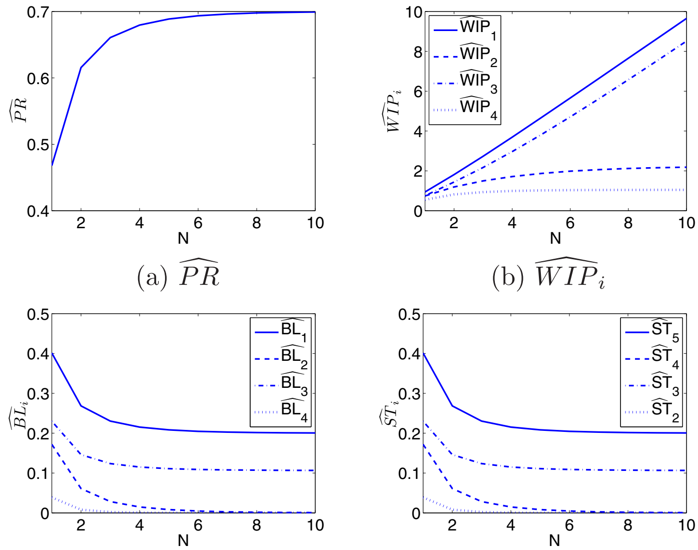

(a) $\widehat{PR}$ (b) $\widehat{WIP}_i$

(c) $\widehat{BL}_i$ (d) $\widehat{ST}_i$

Figure 4.17: Performance of Line L_7 ("oscillating" machine efficiency allocation)

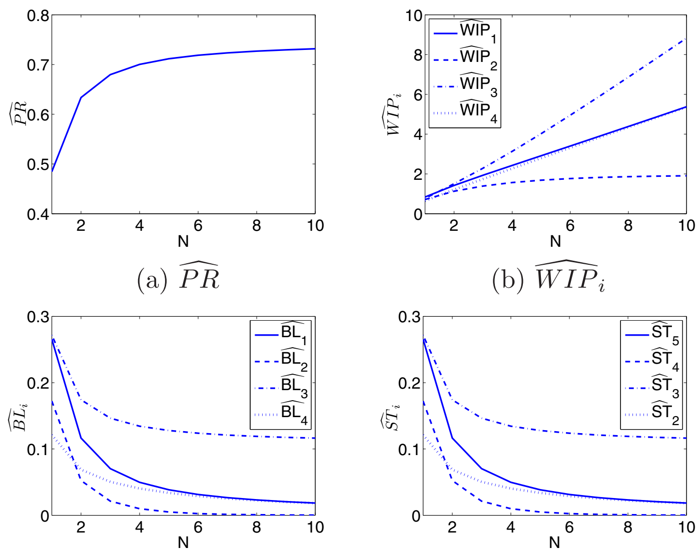

(a) $\widehat{PR}$ (b) $\widehat{WIP}_i$

(c) $\widehat{BL}_i$ (d) $\widehat{ST}_i$

Figure 4.18: Performance of Line L_8 (good machine surrounded by low efficiencies ones)

Analytical investigation: Consider the joint probability $P_{i,\ldots,j}[h_i,\ldots,h_j]$ that buffers i, $i+1$, …, j, contain h_i, h_{i+1}, …, h_j parts, respectively. In general, this joint probability is not close to the product of its marginals, i.e.,

$$P_{i,\ldots,j}[h_i,\ldots,h_j] \neq P_i[h_i]P_{i+1,\ldots,j}[h_{i+1},\ldots,h_j],$$

where $P_i[h_i]$ is the probability that the i-th buffer contains h_i parts. However, it turns out that for certain values of h_i, …, h_j, related to blockages and starvations, these probabilities are indeed close to each other. Specifically, define

$$\begin{aligned} \delta_{ij}(b) &:= |P_{i,\ldots,j}[0,b,N_{i+2},\ldots,N_j] - P_i[0]P_{i+1,\ldots,j}[b,N_{i+2},\ldots,N_j]|, \\ \delta^{ij}(a) &:= |P_{i,\ldots,j}[a,N_{i+1},\ldots,N_j] - P_i[a]P_{i+1,\ldots,j}[N_{i+1},\ldots,N_j]|, \\ & \quad 1 \leq b \leq N_{i+1}, \qquad 1 \leq a \leq N_i \end{aligned}$$

and

$$\delta := \max_{i,j} \max_{a,b} \{\delta_{ij}(b), \delta^{ij}(a)\}. \tag{4.44}$$

Extensive numerical simulations show that δ is practically always small. An illustration is given in Table 4.1 for several four-machine lines with $N_i = 3$, $i = 1, 2, 3$.

Table 4.1: Illustration of δ

p_1	p_2	p_3	p_4	δ
0.80	0.80	0.80	0.80	0.0073
0.70	0.80	0.70	0.80	0.0233
0.70	0.90	0.70	0.90	0.0568
0.60	0.99	0.99	0.60	0.1181
0.99	0.60	0.60	0.99	0.0083

Thus, we formulate

Numerical Fact 4.1 *For Bernoulli lines defined by assumptions (a)-(e),*

$$\delta \ll 1.$$

Based on this fact, the following can be proved:

Theorem 4.3 *For Bernoulli lines defined by assumptions (a)-(e), the accuracy of the production rate estimate is characterized by*

$$|\widehat{PR}(p_1,\ldots,p_M,N_1,\ldots,N_{M-1}) - PR(p_1,\ldots,p_M,N_1,\ldots,N_{M-1})| = O(\delta),$$

where δ is defined by (4.44) and $O(\delta)$ denotes a quantity of the same order of magnitude as δ.

Proof: See Section 20.1.

Numerical investigation: The accuracy of the performance measure estimates (4.36)-(4.40) has been investigated numerically using a C++ code, which simulates production lines defined by assumptions (a)-(e). (This code is included in the **Simulation** function of the PSE Toolbox – see Section 19.9.) Since similar numerical investigations are carried out throughout this textbook, we define them below by a standard procedure.

Simulation Procedure 4.1:

(1) Select the initial status of each machine up with probability p_i and down with probability $1 - p_i$, $i = 1, \ldots, M$.

(2) For each line under consideration, carry out 20 runs of the simulation code.

(3) In each run, use the first 20,000 time slots as a warm-up period and the subsequent 400,000 time slots to statistically evaluate PR, WIP_i, ST_i and BL_i. This results in 95% confidence intervals of less than 0.001 for PR; 0.02 for WIP_i; and 0.002 for ST_i and BL_i.

■

The accuracy of the estimates has been evaluated by

$$\epsilon_{PR} = \frac{|\widehat{PR} - PR|}{PR} \cdot 100\%, \tag{4.45}$$

$$\epsilon_{WIP_i} = \frac{|\widehat{WIP}_i - WIP_i|}{N_i} \cdot 100\%, \quad i = 1, \ldots, M-1, \tag{4.46}$$

$$\epsilon_{ST_i} = |\widehat{ST}_i - ST_i|, \quad i = 2, \ldots, M, \tag{4.47}$$

$$\epsilon_{BL_i} = |\widehat{BL}_i - BL_i|, \quad i = 1, \ldots, M-1. \tag{4.48}$$

The results of this numerical investigation for the set of production lines (4.43) are shown in Figures 4.19 - 4.21. From this information, the following conclusions can be derived:

- In general, $\widehat{PR}$ provides a relatively accurate estimate of PR; in most cases, the error is within 1% and the largest error is about 3%.
- The accuracy of $\widehat{WIP}_i$, $\widehat{ST}_i$, and $\widehat{BL}_i$ is typically lower.
- The highest accuracy of all estimates is for the uniform machine efficiency pattern.
- The lowest accuracy is for the inverted bowl and "oscillating" patterns.
- Lines, which are inverse of each other, result in identical accuracy of all estimates.

In spite of this accuracy limitation, formulas (4.36)-(4.40) provide a useful analytical tool for performance evaluation of Bernoulli lines, especially taking into account that the parameters of the machines are rarely known on the factory floor with accuracy better than 5% - 10%.

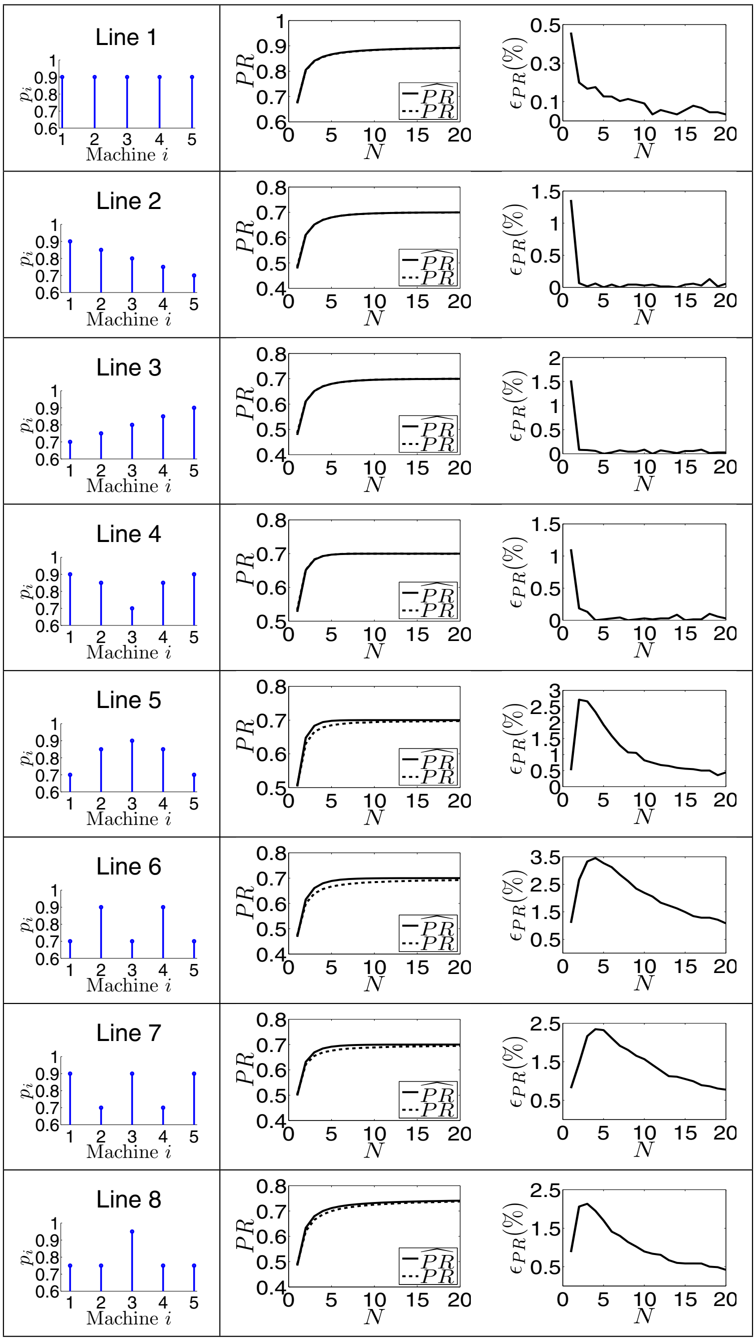

Figure 4.19: Accuracy of $\widehat{PR}$

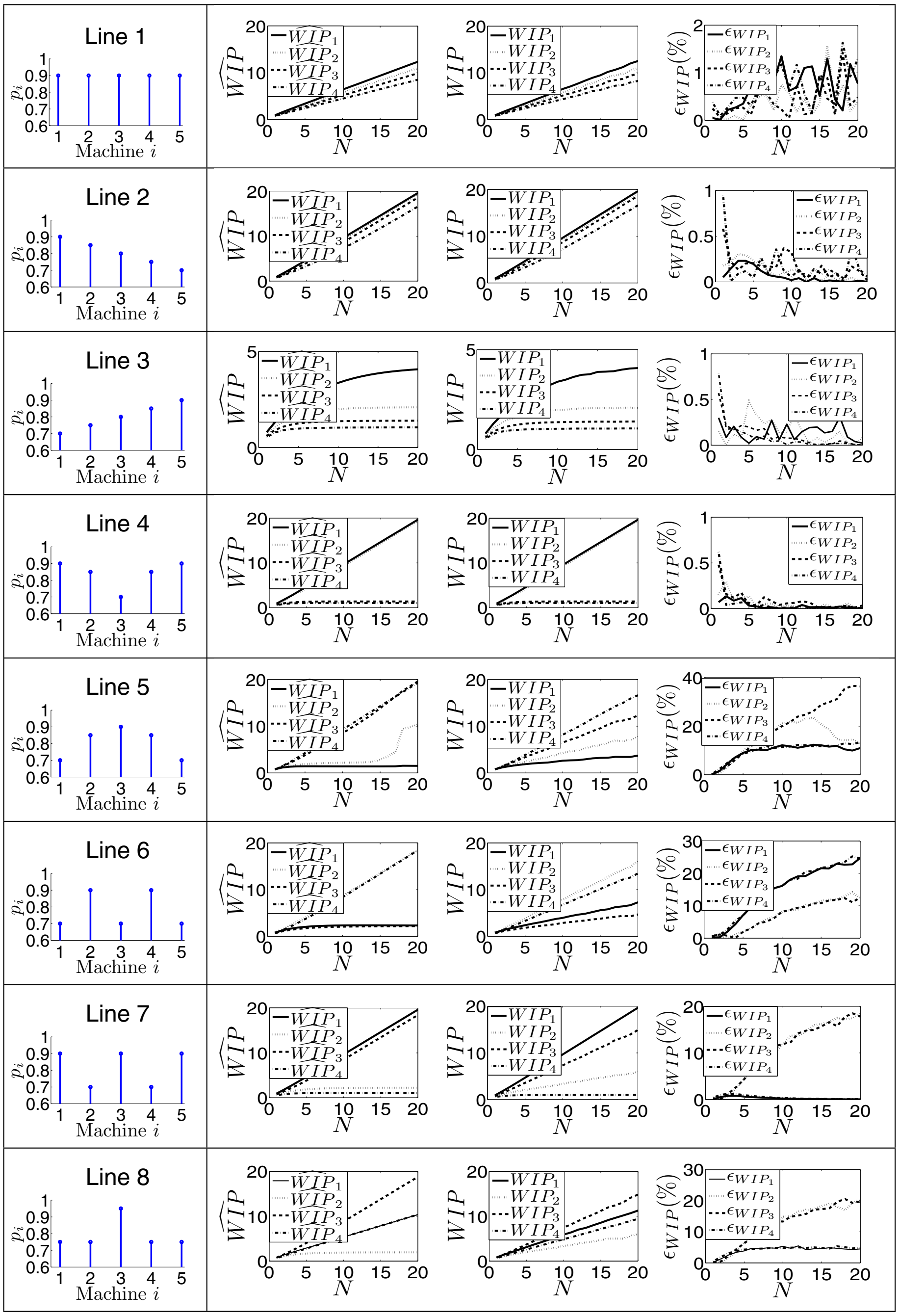

Figure 4.20: Accuracy of $\widehat{WIP}_i$

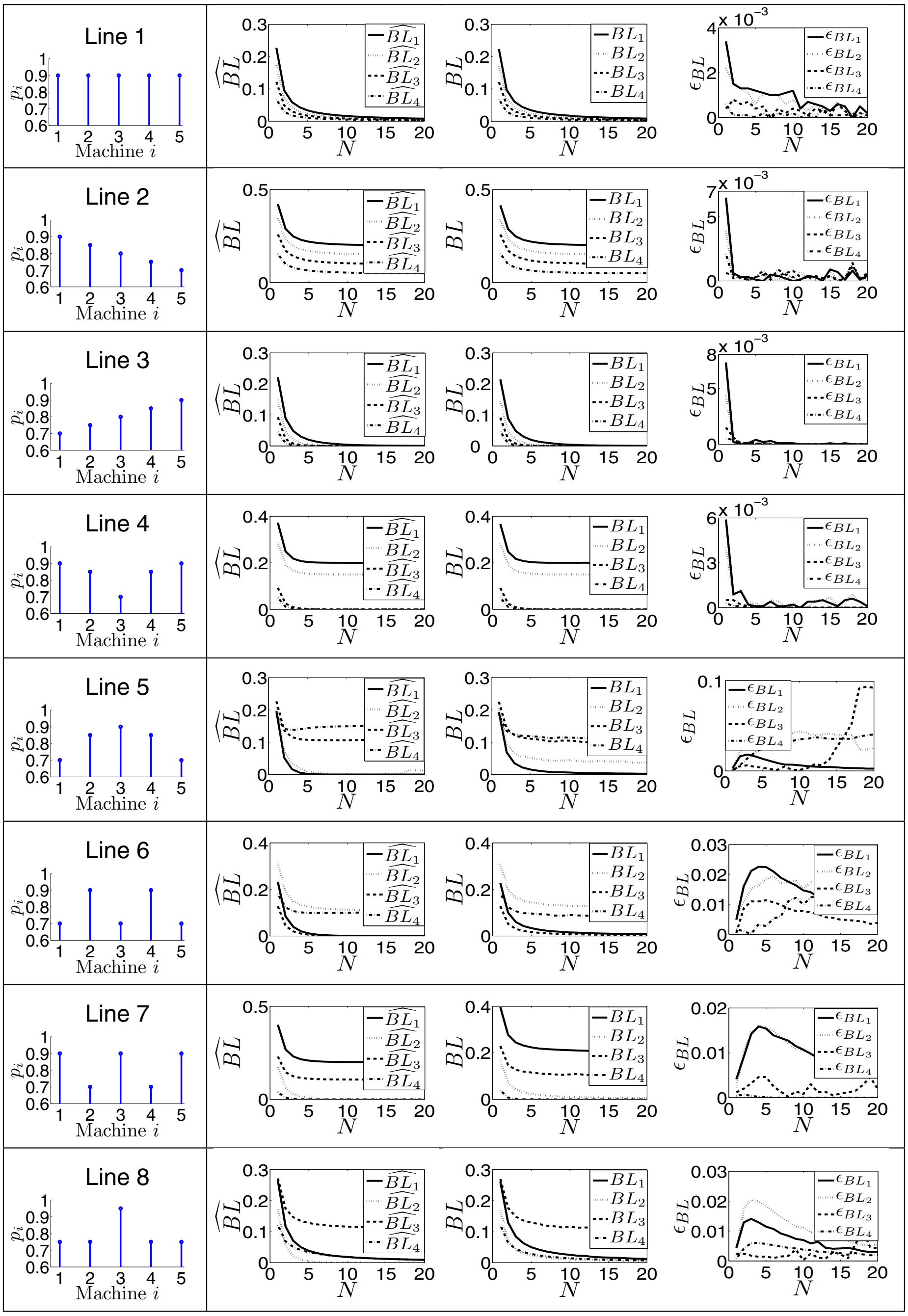

Figure 4.21: Accuracy of $\widehat{BL_i}$

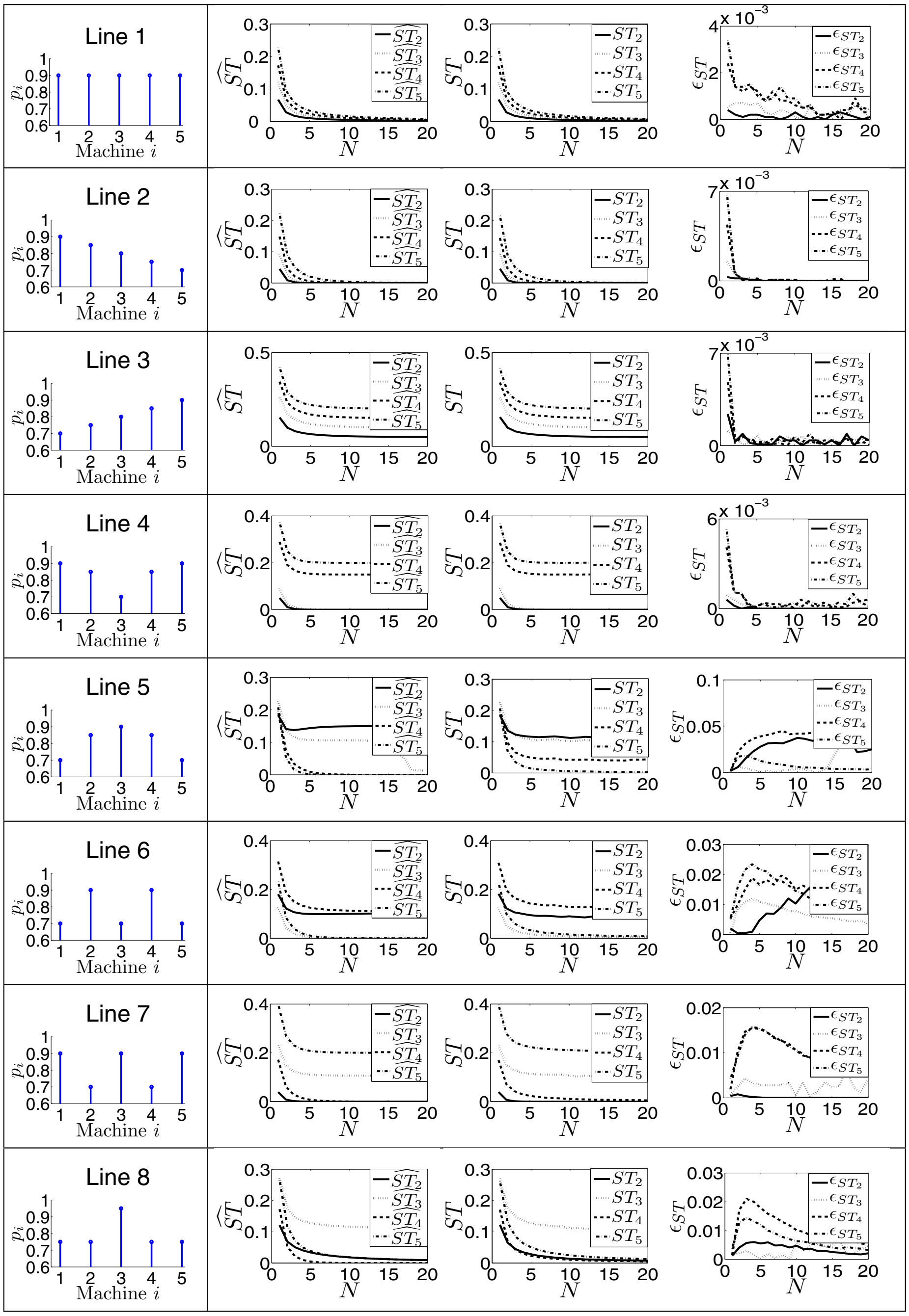

Figure 4.22: Accuracy of $\widehat{ST}_i$

4.3 System-Theoretic Properties

4.3.1 Static laws of production systems

Many engineering systems can be characterized by their *static laws*. For instance, a static law of mechanical systems is:

$$\text{Sum of all forces acting on a rigid body} = 0. \tag{4.49}$$

The statics of electric circuits are described by

$$\text{Sum of currents flowing through a node} = 0 \tag{4.50}$$

and by

$$\text{Sum of all voltage drops and rises in a closed loop} = 0. \tag{4.51}$$

Similarly, the static law of production systems should describe the *steady state flow of parts through this system*. As it has been shown above, in the case of serial lines with Bernoulli machines, this flow is characterized by the steady states of the recursive procedure (4.30), i.e., by

$$\begin{aligned} p_i^b &= p_i[1 - Q(p_{i+1}^b, p_i^f, N_i)], \qquad i = 1, \dots, M-1, \\ p_i^f &= p_i[1 - Q(p_{i-1}^f, p_i^b, N_{i-1})], \qquad i = 2, \dots, M. \end{aligned} \tag{4.52}$$

In the same manner as (4.49)-(4.51) characterize static behavior of mechanical and electrical systems, (4.52) characterizes static properties of the production systems under consideration. Analyzing (4.52), and taking into account the expressions for the performance measures (4.36)-(4.40), we derive below two *system-theoretic properties* of serial lines with Bernoulli machines – *reversibility* and *monotonicity*. One more property – *improvability* – is analyzed in Chapter 5.

4.3.2 Reversibility

Consider a serial line L, defined by assumptions (a)-(e) of Subsection 4.2.1, and its reverse L_r (see Figure 4.23).

Theorem 4.4 *The performance measures of a Bernoulli serial line, L, and its reverse, L_r, are related as follows:*

$$\begin{aligned} &\widehat{PR}^L = \widehat{PR}^{L_r}, \\ &\widehat{BL}_i^L = \widehat{ST}_{(M-i+1)^r}^{L_r}, \qquad i = 1, \dots, M-1. \end{aligned}$$

Proof: See Section 20.1.

The reversibility property of production lines has practical implications. Several of them are mentioned below.

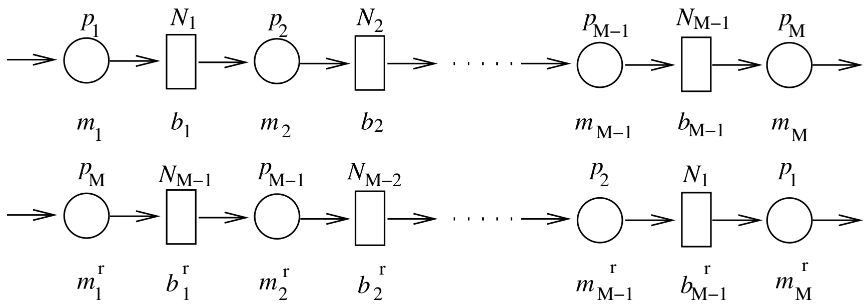

Figure 4.23: M-machine production line and its reverse

- Some argue that buffers at the end of the line should be larger than those at its beginning, since more work has been put into parts as they progress further along the line and are closer to being complete. The reversibility property says that the same effect can be ensured by reversing this argument. Thus, the argument of "end of the line" or "beginning of the line" is not valid for buffer capacity assignment.
- If the machines are identical and only one buffer is available, where should it be placed within the line so that the production rate is maximized? If it is placed anywhere but in the *middle of the line* (assuming the number of machines is even), as it follows from Theorem 4.4, the buffer will be under utilized either in L or in L_r. Thus, the optimal position is the middle of the line. Improvement due to this positioning might be substantial. For instance, consider a 6-machine Bernoulli serial line when $p_i = 0.9$, $i = 1, \dots, 6$ and a single buffer of capacity 2 available for placement within this line. If it is placed as either b_1 or b_5, the resulting production rate is 0.668, whereas placing it in the middle of the line (i.e., as b_3) gives $PR = 0.694$, a 3.8% improvement.
- If all machines and buffers are identical and one machine can be improved, which one should it be, so that the production rate of a serial line with an odd number of machines is maximized? Similar to the above, the reversibility property leads to a conclusion that it should be the machine in the *middle of the line.*
- If all machines are identical and the total buffering capacity N^* must be allocated among $M - 1$ buffers, how should their capacity be selected so that the production rate is maximized? The reversibility property tells us that the allocation, whatever it may be, must be symmetric with respect to the middle machine (if the number of machines is odd) or with respect to the two middle machines (if the number of machines is even). So, the only question that remains is whether the buffers should be of equal capacity or not (assuming that N^* is divisible by M). It is easy to show that buffers of equal capacity do not maximize PR. Therefore, due to the reversibility property and the argument of the first bullet above, optimal

allocation must be of an inverted bowl shape, i.e., larger buffers are in the middle of the line. This result is intuitive, since the machines at the beginning and the end of the line experience less perturbations (because the first machine is not starved and the last is not blocked) and, therefore, need less protection than those in the middle of the line. In practical terms, however, the "bowl effect" is not very significant: the difference of PRs under the uniform and the optimal bowl allocation is typically within 1% (which is often below the accuracy with which parameters of the machines are known). To illustrate this fact, consider a Bernoulli 5-machine line with $p_i = 0.9$. Its production rate for the uniform allocation of $N^* = 20$ is 0.8666, while according to the best bowl allocation, it is 0.8667.

4.3.3 Monotonicity

Could PR of a serial line decrease if the machines or buffers are improved? Intuitively, it is clear that this should not happen. A formal statement to this effect follows from (4.52):

Theorem 4.5 *In Bernoulli serial lines, defined by assumptions (a)-(e) of Subsection 4.2.1,* $\widehat{PR} = \widehat{PR}(p_1, \ldots, p_M, N_1, \ldots, N_{M-1})$ *is*

- *strictly monotonically increasing in* N_i, $i = 1, \ldots, M-1$;
- *strictly monotonically increasing in* p_i, $i = 1, \ldots, M$.

Proof: See Section 20.1.

4.4 Case Studies

4.4.1 Automotive ignition coil processing system

Model validation: The Bernoulli model of this system is obtained in Subsection 3.10.1 and shown in Figure 3.31 for Periods 1 and 2. To validate this model (as well as the model of the next subsection), we use the following procedure:

- Using expressions (4.36)-(4.40), calculate the production rate estimate $\widehat{PR}$ (parts/cycle).
- Keeping in mind that the cycle time, τ, is 6.4 sec for Period 1 and 6.07 sec for Period 2, convert $\widehat{PR}$ into $\widehat{TP}$ (parts/hour):

$$\widehat{TP} = \frac{3600}{\tau}\widehat{PR} \text{ parts/hour.}$$

- Using the throughput measured on the factory floor, TP_{meas}, evaluate the accuracy of the model in terms of the error

$$\epsilon_{TP} = \frac{|\widehat{TP} - TP_{meas}|}{TP_{meas}} \cdot 100\%. \tag{4.53}$$

The results are given in Table 4.2. Clearly, the fidelity of the model for both periods is sufficiently high. In general, it would be desirable to have more data points for the comparison. However, in this application (as well as in many others) the data is quite limited, but the decision nevertheless has to be made. Therefore, we conclude that the model is validated.

Table 4.2: Model validation data

Data Set	$\widehat{PR}$ (parts/cycle)	$\widehat{TP}$ (parts/hr)	TP_{meas} (parts/hr)	Error (%)
Period 1	0.8267	465	472	1.48
Period 2	0.8143	482	472.6	1.99

Although concrete improvement measures for the system at hand will be developed in Chapters 5 and 6, below we use the model validated to investigate several "what if" scenarios.

Effect of starvations by pallets: The model of Figure 3.31 includes the effect of starvations of Op. 1 by empty pallets (i.e., the terms in parenthesis of p_1). This indicates that the number of pallets in the system is not selected appropriately. It is of interest to know how much the performance would improve if the number of pallets were correct. To answer this question, assume that no starvations of Op. 1 takes place (i.e., eliminate the terms in parenthesis in the expression for p_1) and re-calculate the production rate and throughput of the system. The results are shown in Table 4.3. Since the improvement is just about 1%, the system modification by adjusting the number of pallets is not an effective way for continuous improvement.

Table 4.3: Performance without starvation of Op. 1 for pallets

	$\widehat{TP}$ (parts/hr)	Improvement (%)
Period 1	470	1.08
Period 2	488	1.24

Effect of increasing buffer capacity: The buffers in the system of Figure 3.31 are quite small. It is of interest to know how much the performance would improve if the capacity of all buffers were increased. The answer, given in Table 4.4, indicates that increasing the capacity by 50% leads to about 6% - 7% of throughput improvement, while further increases have practically no effect. Thus, increasing (perhaps, only some of the) buffer capacities may be an effective way for system improvement.

Table 4.4: Performance with increased buffer capacity

% increment in buffers	$\widehat{TP}$ (parts/hr)	Improvement (%)
50	492	5.85
100	498	7.03
200	501	7.75
300	502	7.95

(a). Period 1

% increment in buffers	$\widehat{TP}$ (parts/hr)	Improvement (%)
50	513	6.39
100	518	7.45
200	522	8.22
300	523	8.46

(b). Period 2

Effect of increasing machine efficiency: The worst machine in the model of Figure 3.31 is m_{9-10}. Assuming that p_{9-10} is increased by, say, 3%, 5%, or 10%, what would the performance of the system be? The results are shown in Table 4.5. Clearly, increasing the efficiency of machine m_{9-10} leads to a reasonable improvement in system productivity.

Table 4.5: Performance with increased efficiency of m_{9-10}

% increment in p_{9-10}	$\widehat{TP}$ (parts/hr)	Improvement (%)
3	474	2.10
5	480	3.40
10	494	6.30

(a). Period 1

% increment in p_{9-10}	$\widehat{TP}$ (parts/hr)	Improvement (%)
3	493	2.04
5	499	3.32
10	512	6.12

(b). Period 2

Returning to the exponential model: As it follows from the exp-B transformation (3.38)-(3.40), the efficiency p_{9-10} of the Bernoulli machine m_{9-10} can be increased by either decreasing λ_{9-10} or increasing μ_{9-10} given in Table

3.6. Which one of these routes is preferable? In other words, how much should λ_{9-10} be decreased (i.e., T_{up} of m_{9-10} increased) or how much should μ_{9-10} be increased (i.e., T_{down} of m_{9-10} decreased) so that the desired throughput (see Table 4.5) is obtained? The answer, calculated using (3.39), (3.40) and (4.30)-(4.36), is given in Tables 4.6 and 4.7. Clearly, decreasing T_{down} is more effective than increasing T_{up}.

Table 4.6: Performance with increased uptime of m_{9-10}

To achieve desired $\widehat{TP}$	T_{up}	Increment of uptime (%)
474	19.60	40.44
480	26.38	88.97
494	137.97	888.47

(a). Period 1

To achieve desired $\widehat{TP}$	T_{up}	Increment of uptime(%)
493	21.84	34.96
499	28.07	73.47
512	84.52	422.38

(b). Period 2

Table 4.7: Performance with decreased downtime of m_{9-10}

To achieve desired $\widehat{TP}$	T_{down}	Decrement of downtime (%)
474	1.18	25.11
480	0.91	42.24
494	0.28	82.17

(a). Period 1

To achieve desired $\widehat{TP}$	T_{down}	Decrement of downtime (%)
493	1.53	25.59
499	1.19	42.08
512	0.39	80.87

(b). Period 2

4.4.2 Automotive paint shop production system

Model validation: The mathematical model of the paint shop system is shown in Figure 3.34 and the machines' efficiency for five monthly periods is given in Table 3.10. To validate this model, we evaluate its production rate, using expressions (4.36)-(4.40), and compare it with that measured on the factory floor (using (4.53)). The results are shown in Table 4.8. As it follows from this table, the model predicts well the system's performance in all periods except for period 2. This discrepancy is attributed to the fact that during this period a new car model was introduced and, perhaps, some transient phenomena played a substantial role. Thus, omitting period 2, we assume that the model is validated.

Table 4.8: Model validation data (jobs/hour)

	Time Month 1	Time Month 2	Time Month 3	Time Month 4	Time Month 5
$\widehat{TP}$	54.10	53.63	54.81	54.33	55.48
TP_{meas}	53.5	43.81	51.27	54.28	55.89
Error	1.12%	22.41%	6.90%	0.09%	-0.73%

Effect of starvations by carriers: The model of Figure 3.34 and Table 3.13 includes the effect of starvations of Op. 3 by lacking carriers (the terms of p_3 in parenthesis). Deleting these terms and re-calculating the production rate, we determine the effect of the starvations. The results are given in Table 4.9. Clearly, elimination of starvations by carriers could yield up to 10% improvement in system production rate.

Table 4.9: Performance without starvation of Op. 3 by carriers (jobs/hour)

	Time Month 1	Time Month 2	Time Month 3	Time Month 4	Time Month 5
$\widehat{TP}$	59.29	59.10	58.54	59.78	60.09
Improvement	9.59%	10.20%	6.81%	10.03%	8.31%

Effect of increasing buffer capacity: To investigate this effect, we calculate the production rate of the system with each buffer increased by 50% and by 100%. The results are given in Table 4.10. Clearly, increasing buffer capacity has almost no effect on system production rate.

Effect of increasing machine capacity: As it follows from (3.61), machine efficiency depends on both production losses L_i and machine capacity c_i. While the production losses (due to push button activation) are difficult to eliminate, the speed of the operational conveyors may be modified relatively easily within

Table 4.10: Performance with increased buffer capacity (jobs/hour)

% incre.		Time Month 1	Time Month 2	Time Month 3	Time Month 4	Time Month 5
50	$\widehat{TP}$	54.20	53.71	55.19	54.38	55.61
	Imp.	0.18%	0.15%	0.90%	0.09%	0.23%
100	$\widehat{TP}$	54.22	53.72	55.33	54.38	55.64
	Imp.	0.23%	0.17%	1.15%	0.09%	0.29%

±10% of their nominal values given in Table 3.8. Assuming that this would not lead to a substantial change in L_i's, we calculate the production rate with all operations having the capacity $1.1c_i$. The results are in Table 4.11. Thus, increasing the speed of operational conveyors by 10% leads to over 11% improvement in system throughput.

Table 4.11: Performance with increased machine capacity (jobs/hour)

	Time Month 1	Time Month 2	Time Month 3	Time Month 4	Time Month 5
$\widehat{TP}$	60.39	59.93	61.10	60.63	61.78
Improvement	11.42%	11.75%	11.48%	11.60%	11.36%

4.5 Summary

- For two-machine lines,
  - the probabilities of buffer occupancy can be expressed in closed form as functions of machine and buffer parameters;
  - based on these probabilities, closed form expressions for all performance measures are derived.
- For $M > 2$-machine Bernoulli lines,
  - due to the complexity of Markov chains involved, no closed form expression for the probabilities of buffer occupancy can be derived;
  - however, a recursive aggregation procedure is developed, the steady states of which lead to closed form estimates of all performance measures;
  - the accuracy of these estimates is high for the production rate (typically, within 1%) and lower for work-in-process and blockages/starvations;

  - the accuracy of the estimates for all performance measures depends on the pattern of machine efficiency allocation, with the lowest accuracy taking place for the inverted bowl and "oscillatory" allocations.

- The serial lines under consideration possess the property of reversibility: if the flow of parts is reversed, the production rate remains the same, while the probability of blockage (respectively, starvation) of machine i in the original line becomes the probability of starvation (respectively, blockage) of machine $M - i + 1$ in the reversed line.

- The serial lines under consideration possess the property of monotonicity: improving any machine efficiency or increasing any buffer capacity always leads to an increased production rate of the system.

4.6 Problems

Problem 4.1 Consider a two-machine Bernoulli production line defined by the conventions of Subsection 4.1.1 with $N = 1$ (i.e., machine m_1 serves as the buffer).

(a) Draw the state transition diagram of the ergodic Markov chain that describes this system and determine its transition probabilities.

(b) Calculate the stationary probability of each state of this Markov chain and derive the formula for the production rate of this system.

(c) Assuming that $p_1 = p_2 =: p$, draw the graph of PR as a function of $p \in [0.5, 0.99]$ and comment on the qualitative behavior of this graph.

Problem 4.2 Consider again a two-machine Bernoulli production line defined by conventions (a)-(e) of Subsection 4.1.1.

(a) Assume $p_1 = 0.95$ and $p_2 = 0.6$. Calculate and plot PR, WIP, BL_1 and ST_2 as a function of N for N from 1 to 10. Based on these plots, determine the buffer capacity that is reasonable for this system.

(b) Assume $p_1 = 0.6$ and $p_2 = 0.95$. Again calculate and plot PR, WIP, BL_1 and ST_2 as a function of N for N between 1 and 10. Will your choice of buffer capacity change?

Problem 4.3 Consider a two-machine Bernoulli production line defined by conventions (a)-(e) of Subsection 4.1.1. Assume that $N = 5$ and $p_1 p_2 = 0.81$.

(a) Under this constraint, find p_1 and p_2, which maximize PR. (You may use trial and error to accomplish this; alternatively, you may think a little bit, look at the expressions for the performance measure, make an "educated guess" and verify it by calculations.)

(b) For these p_1 and p_2, calculate PR, WIP, BL_1 and ST_2. What can you say about qualitative features of WIP, BL_1 and ST_2?

(c) Interpret the results and formulate a conjecture concerning the optimal allocation of p_i's.

Problem 4.4 Consider a two-machine Bernoulli production line defined by conventions (a)-(e) of Subsection 4.1.1. Suppose that each machine produces a good part with probability g_i and a defective part with probability $1 - g_i$, $i = 1, 2$. Assume that quality control devices operate in such a manner that a defective part is removed from the system immediately after the machine that produced this part.

(a) Derive expressions for the production rate of good parts and for WIP, BL_1 and ST_2 in this system.
(b) Using any example you wish, check if the reversibility property still holds.

Problem 4.5 Consider a two-machine Bernoulli production line defined by all but one of the conventions of Subsection 4.1.1. Specifically, assume that instead of the blocked before service, the following convention is used: Machine m_1 is blocked during a time slot if it is up at the beginning of this time slot and the buffer is full at the end of the previous time slot (i.e., the blockage of m_1 is independent of the status of m_2). We refer to this convention as *symmetric blocking* since both starvation and blocking conventions are of the same nature - they are defined by the state of the buffer and the status of one machine only. Assume for simplicity that the machines are identical, i.e., $p_1 = p_2 =: p$.

(a) Draw the state transition diagram of the ergodic Markov chain that describes this system and determine the transition probabilities.
(b) Derive the expressions for the stationary probabilities of this Markov chain.
(c) Plot these stationary probabilities for $p = 0.95$ and for $p = 0.55$, assuming that in both cases $N = 5$; compare the resulting graphs with those of Figure 4.4 and explain what are the differences and why they take place.
(d) Derive formulas for PR, WIP, BL_1 and ST_2 as a function of p and N.
(e) Plot PR, WIP, BL_1 and ST_2 as functions of N for N from 1 to 10 and $p = 0.9$; compare the resulting graphs with those of Figure 4.6, Line 1, and explain what are the differences and why they take place.

Problem 4.6 Consider again the two-machine production line with the symmetric blocking as defined in Problem 4.5. Repeat parts (a)-(e) of Problem 4.2, assuming that $p_1 \neq p_2$; for the questions in which numerical values are required, assume that $p_1 = 0.9$ and $p_2 = 0.7$.

Problem 4.7 Investigate if the reversibility property holds for two-machine Bernoulli lines with the symmetric blocking convention defined in Problem 4.5.

Problem 4.8 Repeat Problem 4.3 for a two-machine Bernoulli line with the symmetric blocking convention defined in Problem 4.5.

Problem 4.9 Consider a 5-machine Bernoulli production line defined by conventions (a)-(e) of Subsection 4.2.1.

(a) Assume $p_i = 0.9$, $i = 1, \dots, 5$, and all buffers are of equal capacity. Calculate and plot $\widehat{PR}$, $\widehat{WIP}$, $\widehat{BL}_i$ and $\widehat{ST}_i$ as functions of N_i for $N_i = 1, 2, 3, 4$, and 5. Based on these results, determine the buffer capacity, which is reasonable for this system.

(b) Assume now that $p_i = 0.7$, $i = 1, \dots, 5$, and buffers are as above. Again calculate and plot $\widehat{PR}$, $\widehat{WIP}$, $\widehat{BL}_i$ and $\widehat{ST}_i$ as functions of N_i. Will your choice of buffer capacity change?

(c) Interpret the results. Formulate your conjecture as to the choice of buffer capacity as a function of machine efficiency.

Problem 4.10 Consider a 3-machine Bernoulli production line defined by conventions (a)-(e) of Subsection 4.2.1. Assume $N_i = 1$, $i = 1, 2$, and $p_1p_2p_3 = (0.8)^3$.

(a) Under this constraint, find p_i, $i = 1, 2, 3$, which maximize $\widehat{PR}$. (You may use the trial and error method and the PSE Toolbox to accomplish this.)

(b) For these p_i, calculate $\widehat{WIP}$, $\widehat{BL}_i$ and $\widehat{ST}_i$. What can you say about $\widehat{WIP}$? Interpret the results and formulate a conjecture concerning the optimal allocation of p_i's.

Problem 4.11 Consider the production system of Figure 3.38 and its 5-machine Bernoulli model constructed in Problem 3.3.

(a) Calculate the production rate of this system.

(b) Calculate the average occupancy of each buffer.

(c) Calculate the probabilities of blockages and starvations of all machines.

(d) Assuming that the Bernoulli buffer capacity is increased by a factor of 2, recalculate the production rate. Does it make practical sense to have all buffer capacities increased?

(e) Assume that efficiency of all Bernoulli machines is increased by 10% and again recalculate the production rate. Does it make sense to have all efficiencies increased?

Problem 4.12 Repeat the steps of Problem 4.11 for the Bernoulli model of the production system constructed in Problem 3.4.

Problem 4.13 Consider a seven-machine Bernoulli line with machines having identical efficiency. Assume that two buffers with equal capacities are available to be placed in this system.

(a) Where should the buffers be placed so that $\widehat{PR}$ is maximized?

(b) Suggest an example illustrating the efficacy of your solution.

Problem 4.14 Consider a ten-machine Bernoulli line with machines of identical efficiency and buffers of identical capacity. Assume that the efficiency of two machines can be increased (or new machines with higher efficiency can be purchased).

(a) Which of the machines should be improved (or replaced) so that $\widehat{PR}$ is maximized?

(b) Suggest an example illustrating the efficacy of your solution.

Problem 4.15 Consider an $M > 2$-machine Bernoulli line with the symmetric blocking convention defined in Problem 4.5.

(a) Develop a recursive aggregation procedure for performance analysis of this line.

(b) Derive formulas for estimates of $\widehat{PR}$, $\widehat{WIP}_i$, $\widehat{BL}_i$ and $\widehat{ST}_i$.

Problem 4.16 Using examples, investigate the reversibility property of $M >$ 2-machine Bernoulli lines with the symmetric blocking convention. In particular, investigate if

$$\begin{aligned} \widehat{PR}^{L} &= \widehat{PR}^{L_r}, && (4.54)\\ \widehat{BL}_i^{L} &= \widehat{ST}^{L_r}_{(M-i+1)^r}, \quad i = 1, \dots, M && (4.55)\\ & && (4.56) \end{aligned}$$

still hold and, in addition,

$$\widehat{WIP}^{L_r}_{i^r} = N_{M-i} - \widehat{WIP}^{L}_{M-i}. \tag{4.57}$$

Problem 4.17 Using examples, investigate the monotonicity property of $M > 2$-machine Bernoulli lines with the symmetric blocking convention.

4.7 Annotated Bibliography

The initial analysis of two-machine Bernoulli lines has been carried out in

[**4.1**] J.-T. Lim, S.M. Meerkov and F. Top, "Homogeneous, Asymtotically Reliable Serial Production Lines: Theory and a Case Study," *IEEE Transactions on Automatic Control*, vol. 35, pp. 524-534, 1990.

under the assumption that the machines are asymptotically reliable, i.e., their efficiencies are close to 1. The general case has been addressed in

[**4.2**] D.A. Jacobs and S.M. Meerkov, "A System-Theoretic Property of Serial Production Lines: Improvability," *International Journal of System Science*, vol. 26, pp. 95-137, 1995.

The case of $M > 2$-machine lines has also been analyzed in [4.1] for the asymptotically reliable machines and then generalized in [4.2].

Numerical investigation of aggregation procedure accuracy has been carried out by J. Huang and A. Khondker in the framework of their course project in the class on *Production Systems Engineering*.

The properties of reversibility and monotonicity have been known for a long time. In the framework of serial lines with exponential machines, the reversibility property has been discovered in

[**4.3**] G. Yamazaki and H. Sakasegawa, "Property of Duality in Tandem Queueing Systems," *Annals of the Inst. of Statistical Math.*, vol. 27, pp. 201-212, 1975,

while the monotonicity property has been proven to exist in

[**4.4**] J.G. Shanthikumar and D.D. Yao, "Monotonicity and Concavity Properties in Cyclic Queueing Networks with Finite Buffers," in *Queueing Networks with Blocking*, eds. H.G. Perros and T. Altiok, North-Holland, pp. 325-345, 1989.

For the case of Bernoulli lines, these properties have been investigated in

[**4.5**] D.A. Jacobs and S.M. Meerkov, "Mathematical Theory of Improvability for Production Systems," *Mathematical Problems in Engineering*, vol. 1, pp. 95-137, 1995.